

# BIL7 enhances plant growth by regulating the transcription factor BIL1/BZR1 during brassinosteroid signaling<sup>‡</sup>

Tomoko Miyaji<sup>1,†</sup>, Ayumi Yamagami<sup>1,2,†</sup> , Yusuke Nakamura<sup>2</sup>, Kaisei Nishida<sup>2</sup>, Ryo Tachibana<sup>2</sup> , Surina Surina<sup>2</sup>, Shozo Fujioka<sup>1</sup>, Mariano Garcia-Hourquet<sup>3</sup>, Santiago Mora-García<sup>3</sup>, Shohei Nosaki<sup>4,5</sup> , Takuya Miyakawa<sup>2,4</sup> , Masaru Tanokura<sup>4</sup> , Minami Matsui<sup>6</sup> , Hiroyuki Osada<sup>1,7</sup> , Kazuo Shinozaki<sup>1</sup> , Tadao Asami<sup>4,8</sup>  and Takeshi Nakano<sup>1,2,\*</sup> 

<sup>1</sup>RIKEN Center for Sustainable Resource Science, Wako, Saitama 351-0198, Japan,

<sup>2</sup>Molecular and Cellular Biology Laboratory of Totipotency, Graduate School of Biostudies, Kyoto University, Kyoto, Kyoto 606-8502, Japan,

<sup>3</sup>Fundación Instituto Leloir, Av. Patricias Argentinas 435, 1405 Buenos Aires, Argentina,

<sup>4</sup>Department of Applied Biological Chemistry, The University of Tokyo, Yayoi, Bunkyo-ku, Tokyo 113-8657, Japan,

<sup>5</sup>Faculty of Life and Environmental Sciences, University of Tsukuba, Tsukuba, Ibaraki 305-8572, Japan,

<sup>6</sup>Synthetic Genomics Research Group, RIKEN Center for Sustainable Resource Science, Tsurumi, Yokohama, Kanagawa 230-0045, Japan,

<sup>7</sup>Institute of Microbial Chemistry (BIKAKEN), Kamiosaki, Shinagawa-ku, Tokyo 141-0021, Japan, and

<sup>8</sup>Kihara Institute for Biological Research, Yokohama City University, Maioka, Totsuka, Yokohama 244-0813, Japan

Received 17 May 2024; revised 3 December 2024; accepted 5 December 2024.

\*For correspondence (e-mail [nakano.takeshi.6x@kyoto-u.ac.jp](mailto:nakano.takeshi.6x@kyoto-u.ac.jp)).

<sup>†</sup>These authors contributed equally to this work.

<sup>‡</sup>We dedicate this paper to the memory of Dr. Joanne Chory.

## SUMMARY

Brassinosteroids (BRs) are plant steroid hormones that regulate plant development and environmental responses. BIL1/BZR1, a master transcription factor that regulates approximately 3000 genes in the BR signaling pathway, is transported to the nucleus from the cytosol in response to BR signaling; however, the molecular mechanism underlying this process is unknown. Here, we identify a novel BR signaling factor, BIL7, that enhances plant growth and positively regulates the nuclear accumulation of BIL1/BZR1 in *Arabidopsis thaliana*. BIL7-overexpressing plants were resistant to the BR biosynthesis inhibitor Brz and taller than wild-type (WT) plants were due to increased cell division. BIL7 is mainly localized to the plasma membrane, but during the early stages of cell growth, it was also localized to the nucleus. BIL7 was directly phosphorylated by the kinase BIN2, and nuclear localization of BIL7 was enhanced by the BIN2 inhibitor bionin. BIL7 was found to bind to BIL1/BZR1, and nuclear accumulation of BIL1/BZR1 was strongly enhanced by BIL7 overexpression. Finally, double overexpression of BIL1/BZR1 and BIL7 led to greatly elongated hypocotyls in the presence of Brz. These findings suggest that BIL7 mediates nuclear accumulation of BIL1/BZR1, which activates inflorescence elongation in plants via BR signaling.

**Keywords:** brassinosteroid, signaling pathway, BIL1/BZR1, BIN2, nuclear localization, plant growth, NRPM.

## INTRODUCTION

Brassinosteroids (BRs) are plant hormones essential for plant growth and development. BR-deficient mutants exhibit dwarf phenotypes (Li et al., 1996; Li & Chory, 1997). Most dwarf phenotypes of BR biosynthesis mutants can be rescued by exogenous BR treatment. These findings indicate that BRs play essential roles in plant development.

BRs are perceived at the plasma membrane by the receptor kinase BRASSINOSTEROID INSENSITIVE1 (BRI1) and its coreceptor BRI1-ASSOCIATED RECEPTOR KINASE1 (BAK1)

(Kinoshita et al., 2005; Li et al., 2002; Santiago et al., 2013; Wang et al., 2001). BR-activated BRI1 subsequently activates the phosphatase regulator BRI1 SUPPRESSOR 1 (BSU1) through sequential phosphorylation (Kim et al., 2009; Mora-García et al., 2004; Tang et al., 2008; Wang & Chory, 2006). BSU1 subsequently dephosphorylates and inactivates the kinase BRASSINOSTEROID INSENSITIVE 2 (BIN2), which acts as a negative regulator of BR signaling (Kim et al., 2009; Li & Nam, 2002). BIN2 phosphorylates the transcription factors BIL1/BZR1 (BRZ-INSENSITIVE-LONG

HYPOCOTYL1/BRASSINAZOLE-RESISTANT1) (Asami et al., 2003; He et al., 2005; Wang et al., 2002) and its homolog BRI1-EMS-SUPPRESSOR1 (BES1) (He et al., 2002; Yin et al., 2002, 2005), thereby preventing them from regulating the expression of their target genes.

BR regulates the expression levels of 5000 to 8000 genes (Guo et al., 2013; Sun et al., 2010; Yu et al., 2011). The transcription factor BIL1/BZR1 and its homologs BES1 and BEH1-4 in the BR signal transduction pathway have hundreds of target genes, indicating that the BIL1/BZR1 family proteins play key roles in BR signaling. BIL1/BZR1 is a basic helix–loop–helix (bHLH)-type transcription factor, though it possesses a distinct structure from typical bHLH factors. Structural biology studies have revealed that the BIL1/BZR1 family of TFs contains a bHLH-like DNA-binding domain capable of recognizing both the CACGTG (G-box, specific E-box) element and the CGTG (core of BRRE site) element (Nosaki et al., 2018, 2022), demonstrating the ability to recognize a wide range of binding domains. BIL1/BZR1 function is regulated by phosphorylation and dephosphorylation. In the inactive state of BR signaling, BIL1/BZR1 is phosphorylated and transported to the cytoplasm by 14-3-3 proteins, leading to its subsequent degradation and reduced overall activity (Gampala et al., 2007; Ryu et al., 2007). In the activated state, BIL1/BZR1 is dephosphorylated by PROTEIN PHOSPHATASE 2A (PP2A), stabilizing its activity (Sun et al., 2010; Tang et al., 2011; Yu et al., 2011). Dephosphorylated BIL1/BZR1 accumulates in the nucleus, where it binds to the promoters of downstream BR-regulated genes, modulating their transcription. Furthermore, upon activation, BIL1/BZR1 translocates to the nucleus and controls the expression of target genes by binding to specific DNA-binding sequences. Translocation of BIL1/BZR1 from the cytosol to the nucleus is a crucial step in the BR signal transduction pathway. However, much about the regulatory mechanisms of BIL1/BZR1, especially on how its nuclear localization is regulated, remains unknown. Recently, a novel factor, the scaffold protein RECEPTOR FOR ACTIVATED C KINASE 1 (RACK1), was reported to be involved in the nuclear translocation of BIL1/BZR1 (Li et al., 2023). However, the underlying molecular mechanisms are unclear.

Here, we provide evidence that the novel signaling factor BIL7 promotes nuclear localization of BIL1/BZR1, thereby promoting plant growth. We used a screening system with Brz, a specific inhibitor of the BR biosynthetic enzyme encoded by *DWARF4* (*DWF4*) (Asami & Yoshida, 1999), to identify BIL7 as a novel positive regulator of BR signaling in *Arabidopsis thaliana*. BIL7 was phosphorylated by BIN2 kinase. Treatment with the BIN2 inhibitor bikinin increased the nuclear localization of BIL7. Nuclear accumulation of BIL7 was detected from the transition zone located between the meristem and elongation zone in the roots, coinciding with the region where

BIL1/BZR1 nuclear translocation was observed to be enhanced. Furthermore, considering the induced nuclear localization of BIL1 in *bil7-1D*, it is conceivable that BIL7 is involved in regulating the nuclear translocation of BIL1/BZR1 in the BR signaling pathway.

## RESULTS

### Identification of BIL7, which positively regulates BR signaling

To identify novel factors involved in BR signaling, we screened 8000 full-length cDNA overexpressor (FOX) hunting system lines in *Arabidopsis* (Ichikawa et al., 2006) and identified *Brz-insensitive-long hypocotyl7-1D* (*bil7-1D*), which exhibited significantly longer hypocotyls than WT plants and hypocotyls similar to those of *bil7-1D/bzr1-1D* (Asami et al., 2003; He et al., 2005; Wang et al., 2002) when grown on medium containing Brz in the dark (Figure 1A,B). To identify the causal gene of the *bil7-1D* mutant, we performed PCR amplification and sequencing of the FOX fragment from *bil7-1D* genomic DNA using specific primers; the results revealed insertion of cDNA encoding *At1g63720* in the *bil7-1D* mutant. Significant overexpression of *At1g63720* in *bil7-1D* plants compared with that in WT plants was validated by qRT-PCR (Figure S1A). To confirm that *At1g63720* overexpression is responsible for the *bil7-1D* phenotype, we generated transgenic plants expressing the *At1g63720* CDS driven by cauliflower mosaic virus (CaMV) 35S promoter in WT plants (Figure S1A). When the plants were grown on a medium containing Brz in the dark, the *At1g63720*-overexpressing plants exhibited a long hypocotyl phenotype similar to that of *bil7-1D* (Figure 1A, B). Therefore, we identified this gene as a causal gene and named it *BIL7*. *BIL7* encodes a novel protein that contains putative nuclear localization signal (NLS) sequences but no other known functional domains (Figure S2A). *BIL7* has three homologs in *Arabidopsis*, named *BIL-seven-homologs* (*BSHs*) (Figure S2A), and homologs in many other plant species (Figure S2B,C).

To elucidate the functional role of BIL7 in BR signaling, we investigated the downstream events of BR signaling in BIL7-overexpressing plants, BIL7-knockdown plants generated by RNAi, and BIL7-knockout plants. In the *BIL7-RNAi-1* plants grown in the dark for 7 days after the germination, the expression of *BIL7* mRNA was reduced to 44% of WT, and the expressions of *BIL7* homologs mRNA (*BSH1-3*) was reduced to 70–75% of WT (Figure S1B). Brassinolide (BL) treatment and activation of BR signaling cause negative feedback on BR biosynthesis by downregulating the expression of BR biosynthesis genes such as *DWF4* and *CPD*. Similarly, expression of the BR-repressed genes *DWF4* and *CPD* was reduced in *bil7-1D* plants (Figure 1C). In *bil7-1D* and *BIL7-OX1* plants, endogenous levels of the six BR intermediates were lower than those in

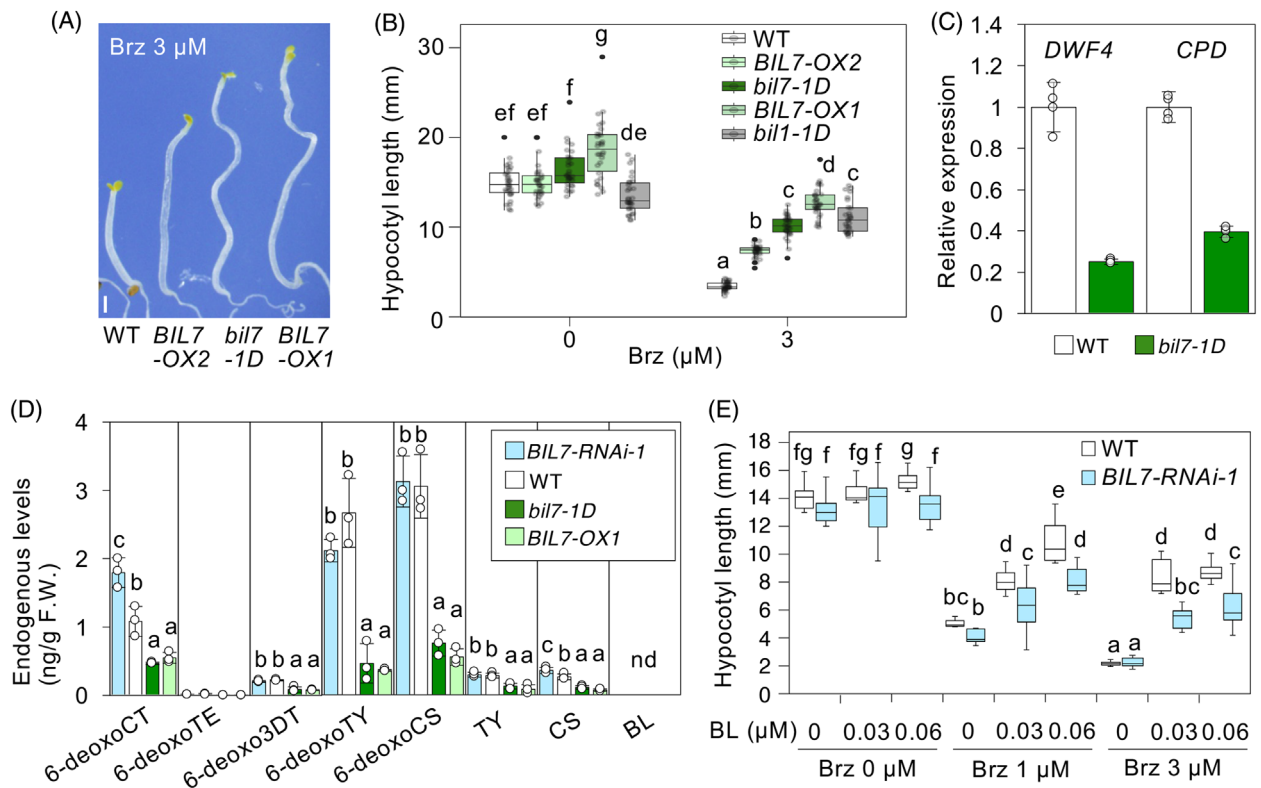


**Figure 1.** BIL7 positively regulates BR signaling. (A) Hypocotyl phenotypes of WT, *35S::BIL7-2 (BIL7-OX2)*, *bil7-1D*, and *35S::BIL7-1 (BIL7-OX1)* plants grown on medium supplemented with 3  $\mu$ M Brz in the dark for 7 days. Scale bars, 1 mm. (B) Hypocotyl lengths of WT, *BIL7-OX2*, *bil7-1D*, *BIL7-OX1*, and *bil1-1D/bzr1-1D* plants grown on medium supplemented with 3  $\mu$ M Brz or mock solution (0  $\mu$ M) in the dark for 7 days. The different letters above the bars indicate statistically significant differences between the samples (two-way ANOVA followed by Tukey–Kramer test,  $P < 0.05$ ;  $n \geq 28$ ). (C) Expression levels of *DWF4* and *CPD* in 27-day-old WT and *bil7-1D* plants. The results are presented as the mean  $\pm$  s.d. ( $n = 3$ ). Each experiment was repeated at least three times with similar results. (D) Endogenous BR content in WT, *BIL7-RNAi-1*, *bil7-1D*, and *BIL7-OX1* plants. The different letters above the bars indicate statistically significant differences between the samples (one-way ANOVA followed by Tukey–Kramer test,  $P < 0.05$ ;  $n = 3$ ). 6-deoxoCT, 6-deoxocathasterone; 6-deoxoTE, 6-deoxoteasterone; 6-deoxo3DT, 3-dehydro-6-deoxoteasterone; 6-deoxoTY, 6-deoxytyphasterol; 6-deoxoCS, 6-deoxocastasterone; BL, brassinolide; CS, castasterone; n.d., not detected; TY, typhasterol. Cathasterone, teasterone, and 3-dehydroteasterone were not detected. (E) Hypocotyl length of WT and *BIL7-RNAi-1* plants grown in the dark for 7 days on medium supplemented with Brz and/or BL. The different letters above the bars indicate statistically significant differences between the samples (three-way ANOVA followed by Tukey–Kramer test,  $P < 0.05$ ;  $n = 15$ ).

WT plants (Figure 1D). These results suggest that BIL7 overexpression activates BR signaling in Arabidopsis. On the other hand, increases in levels of several endogenous BR intermediates were detected in *BIL7-RNAi* plants (Figure 1D). According to the hypocotyl length analysis of plants germinated with Brz and BL in the dark, the *BIL7-RNAi* and *bil7-1* plants exhibited reduced sensitivity to BL (Figure 1E; Figure S3A–C). These results suggest that BIL7 functions as a positive regulator of BR signaling.

### BIL7 regulates plant organ development for plant growth

To characterize the functional role of BIL7 in plant growth, we observed the adult phenotypes of *bil7-1D* and *BIL7-RNAi* plants. Compared with those of WT, the inflorescences of *bil7-1D* plants were approximately 74% longer, with an approximately 43% increase in the number of secondary inflorescences (Figure 2A; Figure S4A,B).

Moreover, the *bil7-1D* plants continued to grow even at 8 weeks after germination, a period when the WT plants had already stopped growing (Figure 2B), similar to what has been observed for Arabidopsis plants that overexpress the BR biosynthesis gene *DWF4* (Choe et al., 2001). Conversely, the inflorescence of *BIL7-RNAi-1* plants, in which BIL7 expression was downregulated, was shorter than that of WT plants (Figure 2A,B). *BIL7-RNAi-2* and *-3* plants in the T1 generation also exhibited a dwarf phenotype similar to that of *BIL7-RNAi-1* (Figure S4C,D). However, *BIL7-RNAi-2* and *-3* were sterile, so it was not possible to utilize *BIL7-RNAi-2* and *-3* plants for expression analysis at the same developmental stage as *BIL7-RNAi-1* plants. Meanwhile, there was no statistically significant difference between the *bil7-1* and WT plants (Figure S3D–F). These results suggest that BIL7 and BSHs function to promote inflorescence elongation.

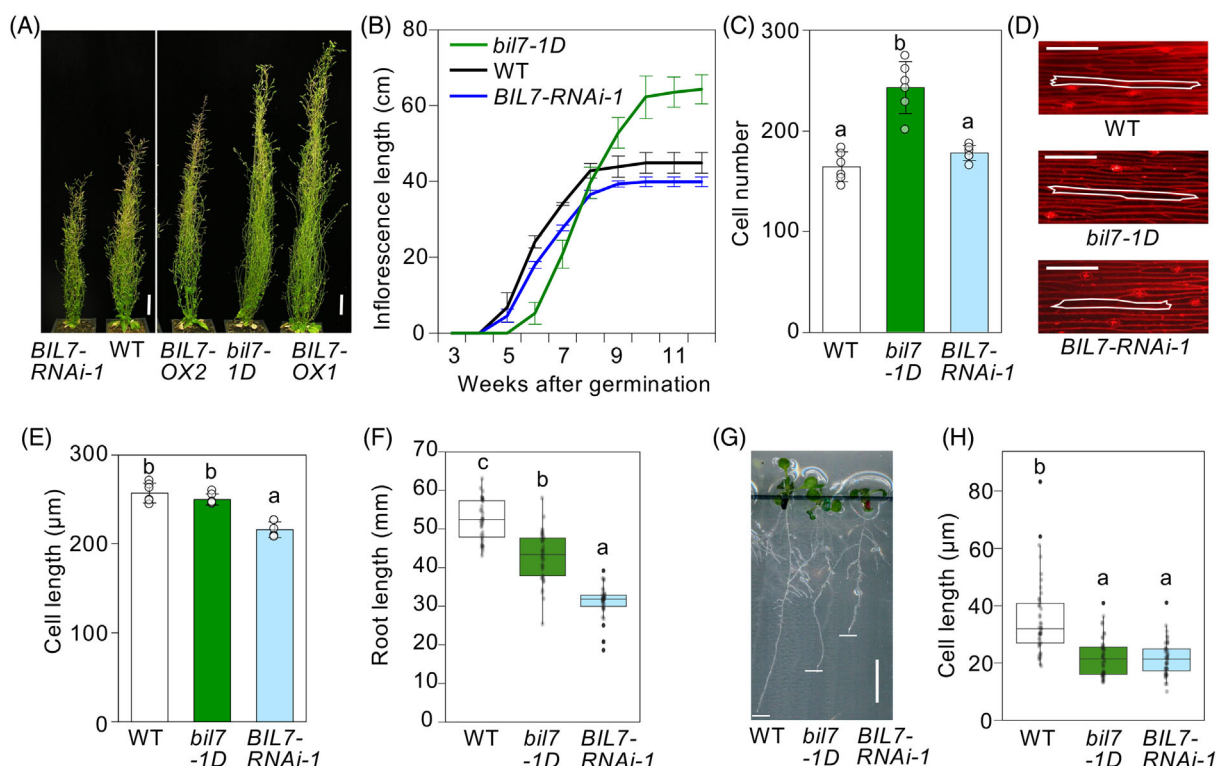


**Figure 2.** BIL7 regulates inflorescence and root elongation.

(A) Phenotypes of *BIL7-RNAi-1*, WT, *BIL7-OX2*, *bil7-1D*, and *BIL7-OX1* plants grown in soil for 63 days. Scale bars, 5 cm.

(B) Inflorescence length of WT, *bil7-1D*, and *BIL7-RNAi-1* plants during development. The results are presented as the mean  $\pm$  s.d. ( $n = 6$ ).

(C–E) Number (C), shape (D), and length (E) of epidermal cells in the primary inflorescences of 91-day-old WT, *bil7-1D*, and *BIL7-RNAi-1* plants. The different letters above the bars indicate statistically significant differences between the samples (one-way ANOVA followed by Tukey–Kramer test,  $P < 0.05$ ;  $n \geq 28$ ). Scale bars, 100  $\mu$ m.

(F–H) Root length (F) and phenotype (G) of the primary roots of 7-day-old plants and cell length (H) in the root transition zones of 4-day-old WT, *bil7-1D*, and *BIL7-RNAi-1* plants grown vertically on  $\frac{1}{2}$  MS medium supplemented with 1.5% sucrose and 0.4% gellan gum. The different letters above the bars indicate statistically significant differences between the samples (one-way ANOVA followed by Tukey–Kramer test,  $P < 0.05$ ;  $K: n \geq 28$ ,  $M: n = 42$ ). Scale bars, 1 cm. The white lines indicate the root tips.

To analyze the ability of BIL7 to regulate inflorescence stem elongation, the number and length of inflorescence epidermal cells were observed via propidium iodide (PI) staining. The *bil7-1D* mutant had more inflorescence epidermal cells than WT (Figure 2C) but the length of these cells did not differ from that of WT (Figure 2D,E). In *BIL7-RNAi-1* inflorescences, cell elongation was reduced in comparison with that in WT plants (Figure 2D, E). Therefore, BIL7 appears to promote both cell division and elongation, at least in the inflorescence. We also examined the effect of BIL7 on root growth. Compared with those of WT, the roots of *BIL7-RNAi-1* were significantly shorter (Figure 2F,G); the cell length of *BIL7-RNAi-1* roots was also significantly shorter (Figure 2H). These results suggest that BIL7 promotes root elongation through cell elongation in the roots. On the other hand, *bil7-1D* also displayed a short-root phenotype (Figure 2F, G). This result is consistent with previous observations that BRs increase root length at low concentrations but decrease it at high concentrations (Clouse et al., 1996; Gonzalez-Garcia et al., 2011). These results suggest that

BIL7 regulates plant inflorescence and root growth by promoting cell elongation and controlling the timing of cell division.

#### BIL7 localizes to the plasma membrane and the nucleus during plant development

To investigate the molecular role of BIL7 in plant organ development, we examined the organ-specific expression patterns of *BIL7*. Plants harboring the  $\beta$ -glucuronidase gene driven by the *BIL7* promoter (*BIL7pro::GUS*) exhibited strong *BIL7* expression during early development in organs such as root tips, juvenile inflorescences and juvenile rosette leaves. However, *BIL7pro::GUS* expression became weaker or decreased in mature organs, such as in elongated inflorescences and expanded rosette leaves (Figure 3A,B; Figure S5). These results suggest that BIL7 plays a role in early development and that expression of these genes might decrease as organs mature.

To analyze the molecular functions of the BIL7 protein in plant cells, we generated transgenic plants expressing the BIL7-GFP and GFP-BIL7 fusion proteins driven by the

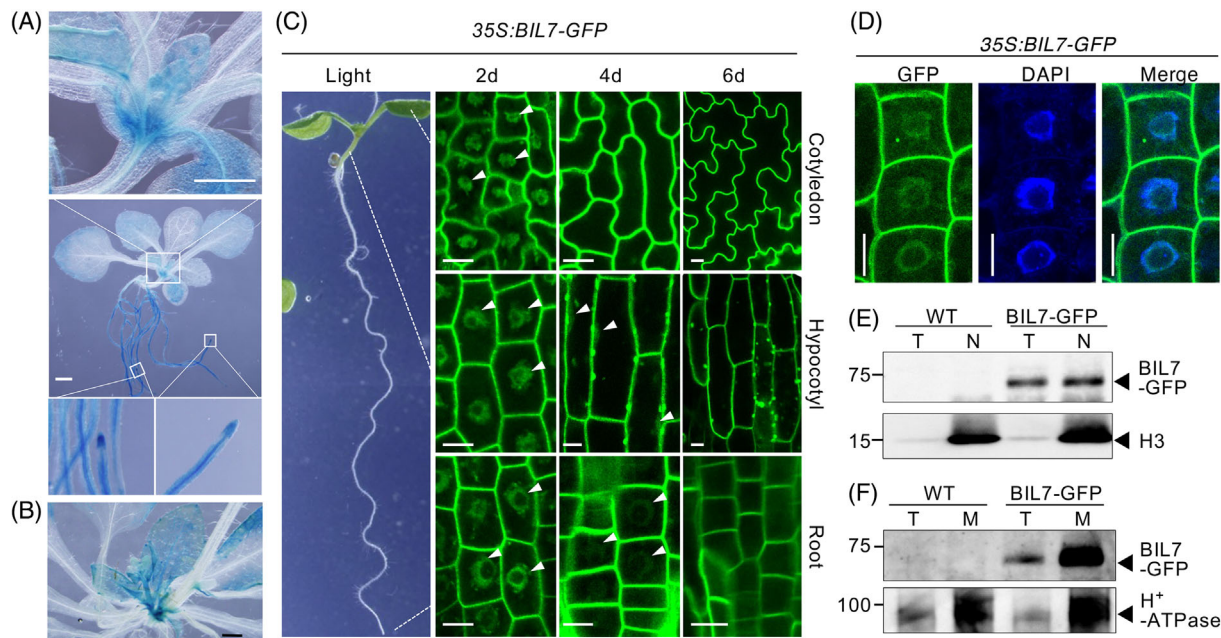


**Figure 3.** Changes in subcellular localization of BIL7 during different stages of development.

(A, B) *BIL7pro::GUS* expression in 14-day-old plants grown in the light (A) and young inflorescences of 40-day-old plants (B). Scale bars, 1 mm.

(C) Subcellular localization of *35S::BIL7-GFP* in epidermal cells of cotyledons and hypocotyls and in the root tips of 2-, 4-, or 6-day-old plants grown in the light. The dashed lines in the left panel indicate the source of the enlargements shown in the right panels. Scale bars, 5  $\mu$ m.

(D) Confocal microscopy images of *BIL7-GFP* transgenic plant root stained with 4',6-diamidino-2-phenylindole (DAPI). DAPI staining indicates the location of the nuclei. Scale bars, 10  $\mu$ m.

(E, F) Immunoblot analyses showing that BIL7-GFP is distributed in the nuclear fraction of 2-day-old seedlings (E) and microsomal fractions of 4-day-old seedlings (F) of WT and *35S::BIL7-GFP* plants. M, microsomal fraction; N, nuclear fraction; T, total extract. Histone H3 (E) and H<sup>+</sup>-ATPase (F) were used as nuclear and microsomal fraction markers, respectively. Full-scan blots are shown in Figure S16.

*CaMV 35S* promoter, and subcellular localization of the BIL7 protein was assessed. All the transformants recapitulated Brz-resistant phenotypes similar to those of the *bil7-1D* mutant, indicating that the BIL7-GFP and GFP-BIL7 proteins are functional (Figure S6). In 2-day-old *BIL7-GFP* plants grown in the light and dark, BIL7-GFP localized to both the nucleus and the plasma membrane in cotyledons, hypocotyls, and roots (Figure 3C; Figure S7A,B). However, the fluorescent signal in the nucleus was significantly decreased in 4- and 6-day-old plants (Figure 3C; Figure S7A). By analyzing *35S::BIL7-GFP* plants via plasmolysis, we confirmed the localization of BIL7-GFP to the plasma membrane (Figure S7B). In *35S::BIL7-GFP* plants, the BIL7-GFP fluorescence signal overlapped with the DAPI signal, which stains genomic DNA in the nucleus. The dark, non-DAPI-stained areas within the nucleus likely correspond to the nucleolus (Figure 3D). To further confirm the subcellular localization of BIL7 by biochemical approaches, we analyzed the subcellular fraction of *35S::BIL7-GFP* plants. Nuclear and microsomal fractions, including the plasma membrane, were prepared from transgenic plants, and the BIL7 protein was analyzed by immunoblotting using an anti-GFP antibody. The BIL7 protein was detected in the nuclear and microsomal fractions (Figure 3E,F).

BIL7 localizes not only to the nucleus but also to the plasma membrane. However, the BIL7 amino acid sequence contains only a short hydrophobic region that does not correspond to a transmembrane region (Figure S8). Other membrane-associated motifs (e.g., those involved in myristoylation and palmitoylation) were not found in BIL7. Searches of the protein lists of Arabidopsis plasma membrane proteomics (Alexandersson et al., 2004; Mitra et al., 2007) and the database for Arabidopsis integral membrane protein (Schwacke et al., 2003) did not yield the AGI code number *At1g63720*.

#### Regulation of BIL7 by BR signaling and the kinase BIN2

To determine the role of BIL7 in BR signaling, the *bil7-1D* mutant was crossed with a BR biosynthesis and signaling mutant. The *bil7-1D* mutant significantly rescued the phenotypes of *bin2-1*, which is a gain-of-function mutant of the BR signaling negative kinase (Li & Nam, 2002), and BR biosynthesis enzyme mutant *det2-1*, indicating short hypocotyls in dark-grown seedlings and dwarf inflorescences (Figure 4A–C; Figure S9A,B). *bil7-1D* clearly rescued the weak BR receptor mutant allele *bri1-5* but could not rescue the null allele *bri1-116* (Figure S9C,D). These results indicate that BIL7 likely acts downstream of BIN2 and that some BR signaling is required for its function.

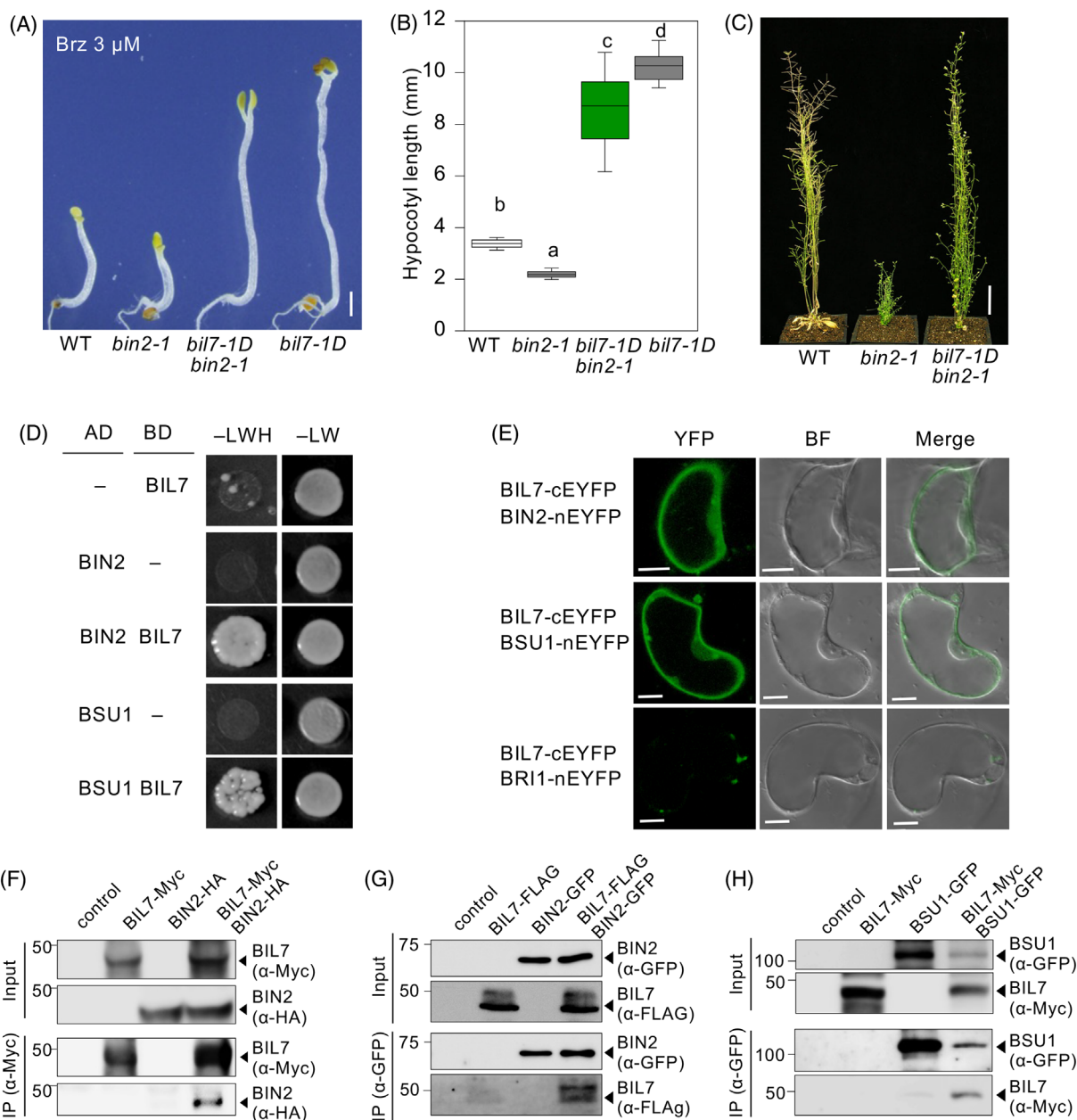


**Figure 4.** BIL7 interacts with BIN2 and BSU1.

(A, B) Hypocotyl phenotypes (A) and hypocotyl length (B) of WT, *bin2-1*, *bil7-1D* *bin2-1* double-mutant, and *bil7-1D* plants germinated on medium supplemented with 3  $\mu$ M Brz in the dark for 7 days. The different letters above the bars indicate statistically significant differences between the samples (one-way ANOVA followed by Tukey–Kramer test,  $P < 0.05$ ;  $n = 30$ ). Scale bars, 1 mm.

(C) Phenotypes of WT, *bin2-1*, and *bil7-1D bin2-1* double mutants grown in soil for 63 days. Scale bars, 5 cm.

(D) Interaction of BIL7 with BIN2 and BSU1 analyzed by Y2H. –LW, synthetic dropout medium (SD) –Leu/–Trp; –LWH, SD –Leu/–Trp/–His; AD, activating domain; BD, binding domain.

(E) Interaction of BIL7 with BIN2 and BSU1 analyzed by a BiFC assay in Arabidopsis suspension cells. BRI1-nEYFP was used with BIL7-cEYFP as a negative control.

(F, G) Interaction of BIL7 with BIN2 analyzed by co-IP in *Nicotiana benthamiana* leaves (F) and in Arabidopsis seedlings grown in the light for 7 days (G).

(H) The interaction of BIL7 with BSU1 in *N. benthamiana* leaves was analyzed by co-IP. The full-scan blots are shown in Figure S16.

As possible relationships between BIL7 and BR signaling emerged from genetic analysis, we searched for BR signaling proteins that interact with BIL7. Yeast two-hybrid (Y2H) assays suggested that BIL7 interacts with BIN2 and

the phosphatase BSU1 (Figure 4D) but not with BRI1 or other intermediate components of the BR signaling pathway (Figure S10). Furthermore, BIL7 interacted with BIN2 and BSU1 both in the nucleus and in the cytosol, as shown

by BiFC assays (Figure 4E; Figure S11). We confirmed the *in vivo* interaction between BIL7 and BIL2 or BSU1 using coimmunoprecipitation (co-IP). First, BIL7-Myc and BIN2-HA were transiently expressed in the leaves of *Nicotiana benthamiana*, after which co-IP was performed. Immunoblotting with anti-Myc and anti-HA antibodies showed that BIL7 coimmunoprecipitated with BIN2 (Figure 4F). Second, we performed co-IP in Arabidopsis double transformants stably expressing BIL7-FLAG and BIN2-GFP, and BIL7-FLAG was coimmunoprecipitated with an anti-GFP antibody (Figure 4G). The interaction of BIL7 with BSU1 was also confirmed by co-IP in *N. benthamiana* (Figure 4H).

Taken together, these results demonstrate that BIL7 interacts with BIN2 and BSU1 both *in vitro* and *in vivo*.

BIN2 is a GSK3-like kinase, and its ability to phosphorylate proteins in plants has been reported (Li & Nam, 2002; Youn & Kim, 2015). Based on the results of possible interactions between BIL7 and BIN2, we performed an *in vitro* kinase assay to determine whether the BIL7 protein was able to be phosphorylated by the BIN2 kinase. After incubating GST-BIN2 and MBP-BIL7 fusion proteins were expressed in and purified from *Escherichia coli*, phosphorylated proteins were detected using Pro-Q Diamond staining. As shown in Figure 5(A), the GST-BIN2 protein did not

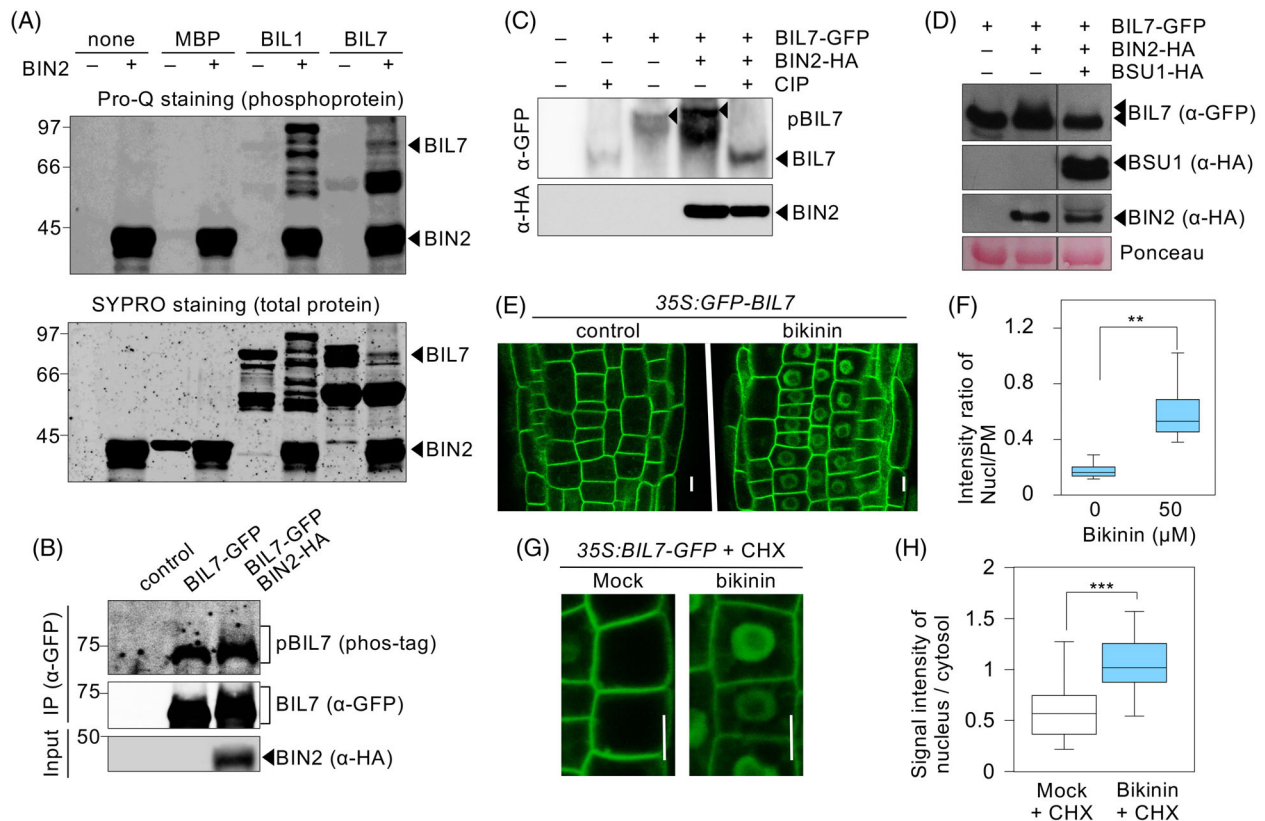


**Figure 5.** The phosphorylation status of BIL7 is regulated by BIN2 and BSU1.

(A) Recombinant BIN2 phosphorylates recombinant BIL7 in an *in vitro* kinase assay. Maltose-binding protein (MBP), MBP-fused BIL1/BZR1, and MBP-fused BIL7 were incubated in the presence (+) or absence (-) of the kinase BIN2. The top and bottom panels show the same gel stained with Pro-Q Diamond (phosphoprotein) and SYPRO Ruby (total protein), respectively.

(B) Phosphorylation status of BIL7 by BIN2 *in vivo*. Proteins from *Nicotiana benthamiana* leaves transiently transformed with the indicated constructs were immunoprecipitated with anti-GFP antibodies, and the immunoblot was probed with phos-tag biotin, anti-GFP, and anti-HA antibodies. The full-scan blots are shown in Figure S16.

(C) Phosphorylation status of BIL7 by BIN2 *in vivo*. Proteins from *N. benthamiana* leaves transiently transformed with the indicated constructs were treated with CIP, separated on a Phos-tag SDS-PAGE gel, and detected by anti-GFP. The slowly migrating band corresponding to BIL7 represents the phosphorylated form of BIL7 (pBIL7). The full-scan blots are shown in Figure S15.

(D) The BIN2-induced mobility shift was eliminated in the presence of BSU1. Proteins from *N. benthamiana* leaves transiently transformed with the indicated constructs were separated via a Phos-tag SDS-PAGE gel and detected via an anti-GFP antibody. The full-scan blots are shown in Figure S15.

(E, F) *35S::GFP-BIL7* plants were grown on 1/2 MS medium for 7 days. Confocal images (E) and quantification of the ratio of nuclear and plasma membrane fluorescence signal intensities (F) of *35S::GFP-BIL7* treated with 50  $\mu$ M bikinin or DMSO (mock control) for 1 h. Scale bars, 5  $\mu$ m. Thirty cells in 3 roots were tested for each dataset. Asterisks indicate a significant difference according to Student's *t*-test (\*\* $P < 0.01$ ).

(G, H) Confocal images (G) and quantification of the ratio of nuclear and cytosolic fluorescence signal intensities (H) of *35S::BIL7-GFP* plants pretreated with 50  $\mu$ M CHX for 30 min and subsequently treated with 50  $\mu$ M CHX and 60  $\mu$ M bikinin or DMSO (mock) for 15 min. Scale bars, 10  $\mu$ m. The results are presented as the mean  $\pm$  s.e. ( $n = 63$  cells). Asterisks indicate a significant difference according to Student's *t*-test (\*\* $P < 0.001$ ).

phosphorylate MBP itself but did phosphorylate the MBP-BIL1/BZR1 protein, which served as a positive control under the same experimental conditions. GST-BIN2 phosphorylated the MBP-BIL7 protein (Figure 5A). We further investigated the phosphorylation status of BIL7 in the presence of BIN2 *in vivo*. BIL7-GFP and BIN2-HA were transiently coexpressed in *N. benthamiana* cells, and the immunoprecipitated BIL7-GFP was analyzed by the Phos-tag biotin, which detects phosphorylated proteins. There was a greater accumulation of phosphorylated BIL7-GFP, a lower electrophoretic mobility form as a high-molecular-weight signal of BIL7, in cells coexpressing BIN2-HA and BIL7 than in cells expressing only BIL7-GFP (Figure 5B). This higher-molecular-weight band of BIL7 was abolished by calf intestine alkaline phosphatase (CIP) treatment (Figure 5C), indicating that the BIL7 mobility shift was due to phosphorylation by BIN2. Taken together, these results suggest that BIN2 directly phosphorylates BIL7. BIL7 interacts not only with BIN2 but also with BSU1, a serine/threonine phosphatase. To analyze the phosphorylation status of BIL7 in the presence of BIN2 and BSU1 in plant cells, BIL7-GFP was transiently coexpressed with BIN2-HA and BSU1-HA in *N. benthamiana*, and phosphorylated BIL7-GFP was detected by an anti-GFP antibody via phos-tag SDS-PAGE. BIN2-induced phosphorylation of BIL7 was reduced by coexpression of BSU1, suggesting that the phosphorylation status of BIL7 might be modulated directly or indirectly by BSU1 (Figure 5D).

Since the nuclear localization of BIL7 was considered altered according to the developmental stage of the plants (Figure 3), we were interested in investigating how BR signaling is involved in the nuclear localization of BIL7. As shown in Figures 4 and 5, the BIL7 protein interacted with and was phosphorylated by BIN2. As a tool to analyze the nuclear localization of BIL7, we used bikinin, which has been identified as a BIN2-inhibitory compound and is widely used in plants (de Rybel et al., 2009). Treatment of *35S::GFP-BIL7* transgenic plants with bikinin induced the nuclear localization of BIL7 (Figure 5E,F). Furthermore, BIL7 was still localized to the nucleus when *35S::BIL7-GFP* plants were treated with bikinin in the presence of the protein synthesis inhibitor cycloheximide (CHX) (Figure 5G,H). These results indicate that BIL7 was translocated to the nucleus in response to the BIN2 inhibitor bikinin. These results suggest that BR signals are transmitted to BIL7 through BIN2 and the inhibition of BIN2 by BR signaling triggers the nuclear localization of BIL7.

#### **BIL7 interacts with BIL1/BZR1 and enhances its nuclear accumulation**

BIL1/BZR1, a master transcription factor involved in BR signaling, is known to be translocated and accumulate in the nucleus after BL treatment (Ryu et al., 2007; Wang et al., 2002). Thus, to examine the relationship between the

nuclear localization of BIL1 and BIL7, the nuclear localization of BIL1/BZR1 and BIL7 was assessed in root tip cells. The development of root cells starts at the quiescent center (QC), and the generated root cells divide into meristem. The root cells in the meristem start to elongate at the transition zone from the meristem to the elongation zone, and root cell elongation continues to increase in the elongation zone (Beemster et al., 2003). In the specific developmental stages of root cells, the fluorescent signals of BIL1/BZR1pro:BIL1/BZR1-YFP in the nucleus were most strongly induced in the transition zone from the meristem to the elongation zone compared to those in the division zone and accumulated further in the elongation zone. (Chaiwanon & Wang, 2015). Thus, to investigate the level of nuclear BIL7 accumulation in roots, we analyzed the localization of BIL7-GFP/GFP-BIL7 expressed under the BIL7 native promoter or *35S* promoter in detail. The nuclear localization of BIL7-GFP was barely detected in the meristem but significantly initiated to increase in the transition zone between the meristem and the elongation zone (Figure 6A; Figure S12). This promoted nuclear localization of BIL7-GFP was maintained even in the early stage of the elongation zone. Hence, the nuclear localization of BIL7 was similar to that of BIL1/BZR1-GFP in the nucleus of root cells.

As the BIL7 protein and BIL1/BZR1 protein were expressed in cells at similar developmental stages and localized to the nucleus, we analyzed the possibility of a direct interaction between BIL7 and BIL1/BZR1. Y2H assays indicated that BIL7 interacted with BIL1/BZR1 (Figure 6B) but not with BES1 (Figure S13A). We used a mutant bil1/bzr1 protein with an altered amino acid sequence that exhibited enhanced protein stability (Wang et al., 2002) and found that this protein interacted more strongly with BIL7 than it did with WT BIL1/BZR1 (Figure S13B). According to BiFC assays, BIL7 interacted with BIL1/BZR1 both in the nucleus and in the cytosol (Figure 6C). In the pull-down assay, a BIL7-interacting signal was detected with BIL1/BZR1, but not with BES1 or the BES1 homologs BEH1-4 (Figure S13C). Furthermore, via a co-IP assay, BIL1/BZR1-Myc was immunoprecipitated by an anti-GFP antibody from lysates of *N. benthamiana* leaves transiently expressing BIL7-GFP and BIL1/BZR1-Myc (Figure 6D). At least two bands corresponding to BIL1/BZR1 with different electrophoretic mobilities were present due to differences in phosphorylation status (Gampala et al., 2007; Ryu et al., 2007). These results suggest that BIL7 interacts equally with phosphorylated and dephosphorylated BIL1/BZR1 in the cytosol and nucleus.

To understand the molecular mechanism of direct interaction between BIL7 and BIL1/BZR1, the effect of BIL7 on the nuclear localization of BIL1/BZR1 was analyzed. By examining the localization of BIL1/BZR1-GFP in plants with varying levels of BIL7 expression, we observed that the

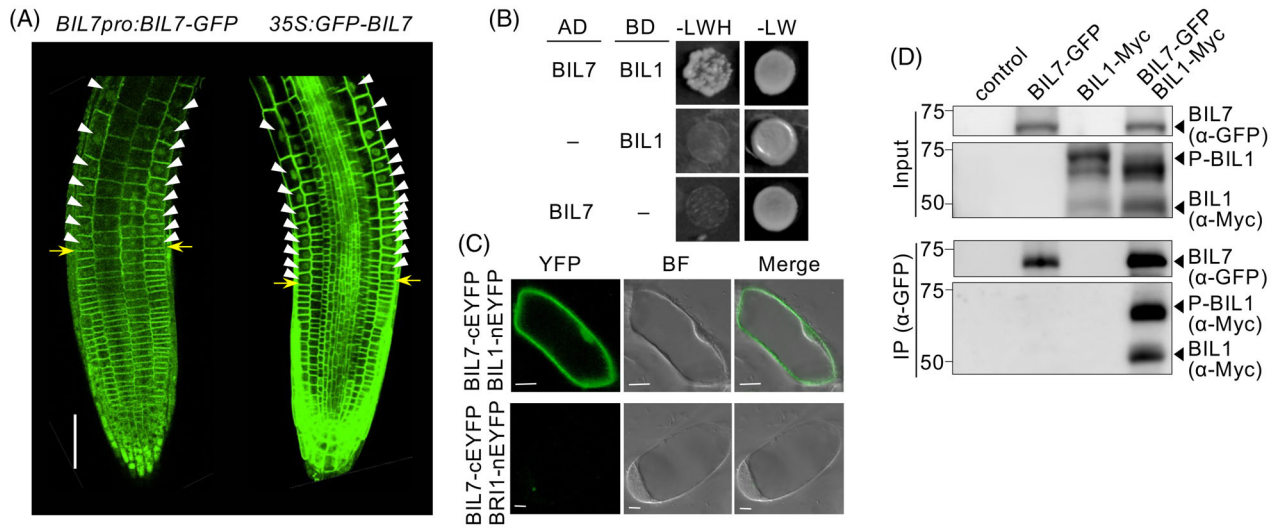


**Figure 6.** BIL7 interacts with BIL1/BZR1.

(A) Confocal images of BIL7-GFP/GFP-BIL7 localization in the root tips of *BIL7*<sub>pro</sub>:*BIL7*-GFP and 35S:*GFP*-*BIL7* plants. Yellow arrows indicate the transition zone between the meristematic zone and the elongation zone of the roots. Arrowheads indicate nuclei with representative GFP signals in the root transition zone. Scale bars, 50 μm.

(B) Y2H analysis of the interaction between BIL7 and BIL1/BZR1.

(C) BiFC analysis of Arabidopsis suspension cells showing the interaction between BIL7 and BIL1/BZR1. BIR1-nEYFP was used with BIL7-cEYFP as a negative control. Scale bars, 10 μm.

(D) co-IP analysis of the interaction between BIL7 and BIL1/BZR1 in *Nicotiana benthamiana* leaves. P-BIL1: phosphorylated BIL1/BZR1. Full-scan blots are shown in Figure S16.

nuclear BIL1/BZR1-GFP signal intensity was markedly stronger in the *bil7-1D* mutant background compared to the WT background. Conversely, a significant reduction of nuclear BIL1/BZR1-GFP signal was detected in the BIL7-RNAi-1 background. (Figure 7A,B). These results indicate that BIL7 promotes nuclear accumulation of the BIL1/BZR1 protein.

The promotion of BIL1/BZR1 dephosphorylation and accumulation of BIL1/BZR1 in the nucleus upon activation of BR signaling have been well-characterized (Gampala et al., 2007; He et al., 2002, 2005; Tang et al., 2011; Wang et al., 2002). Therefore, regulation of BIL1/BZR1 dephosphorylation and nuclear accumulation are important steps in BR signaling, and these two phenomena are considered closely related to each other. We performed immunoblot analysis to examine the phosphorylation status of BIL1/BZR1 in *bil7-1D*, *BIL7*-RNAi, and WT plants. Initially, bikinin treatment increased levels of the amounts of the active and dephosphorylated forms of BIL1/BZR1, which was also observed in the BL-treated BIL1/BZR1 (He et al., 2002). Under the same experimental conditions, *BIL7*-OX plants accumulated more dephosphorylated BIL1/BZR1 forms than the WT plants without bikinin or BL (Figure 7C). Conversely, the accumulation of both the dephosphorylated and phosphorylated BIL1/BZR1 proteins decreased in *BIL7*-RNAi plants. These results suggest that BIL7 promotes the accumulation of dephosphorylated and active forms of the BIL1/BZR1, similar to what occurs in response to BL or bikinin treatment.

Finally, to analyze the biological significance of BIL7 on BIL1/BZR1, the hypocotyl phenotypes of single and double transformants of *BIL7* and *BIL1/BZR1* were examined. Seedlings of 35S:*BIL1/BZR1*-GFP×*bil7-1D* had longer hypocotyls than single 35S:*BIL1/BZR1*-GFP or *bil7-1D* seedlings when grown on medium containing Brz in the dark (Figure S14). Seedlings of 35S:*BIL1/BZR1*-GFP×*BIL7*-RNAi-1 had shorter hypocotyls than single 35S:*BIL1/BZR1*-GFP seedlings with Brz in the dark (Figure S14). Furthermore, the *bil7-1D/bzr1-1D*×*bil7-1D* double mutant had longer hypocotyls than the *bil7-1D/bzr1-1D* plants, which were previously shown to have the most elongated hypocotyls when grown in darkness under Brz conditions (Wang et al., 2002) (Figure 7D,E). These results suggest that the effect of BIL1/BZR1 on hypocotyl elongation is supported and enhanced by BIL7. These results suggest that BIL7 promotes BIL1/BZR1-mediated hypocotyl elongation by possibly enhancing the nuclear accumulation of BIL1/BZR1.

## DISCUSSION

In this study, we identified a novel BIL7 protein from the Arabidopsis mutant *bil7-1D*, which was the strongest phenotype of “*Brz*-insensitive-long hypocotyl” mutants, in relation to a known BR signaling mutant. Although we could not identify an already known functional amino acid domain in the BIL7 protein, analysis of the strongest phenotype during the germination stage and the plant growth-promoting phenotype during the adult growth stage

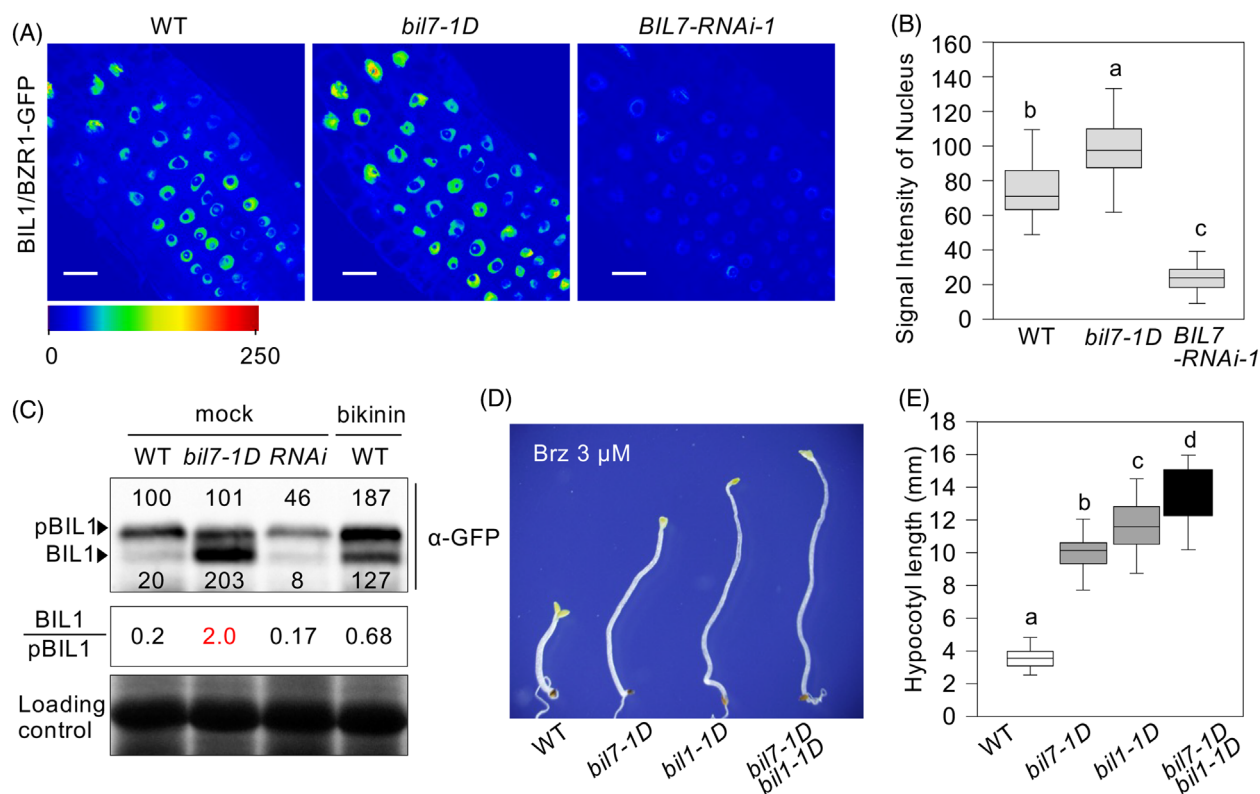


**Figure 7.** BIL7 is involved in nuclear accumulation and increased levels of the dephosphorylated form of BIL1/BZR1.

(A, B) Effect of BIL7 on the nuclear accumulation of BIL1/BZR1-GFP. Fluorescence intensities in roots of WT, *bil7-1D*, and *BIL7-RNAi* plants harboring BIL1/BZR1-GFP grown on 1/2 MS medium supplemented with 1  $\mu$ M Brz for 4 days. Confocal images (A) and quantification of the nuclear fluorescence signal intensity (B). Scale bars, 20  $\mu$ m. Different letters denote significant differences ( $P < 0.05$ ) based on the Tukey–Kramer test. Thirty cells in 3 roots were tested for each dataset. (C) Transgenic seedlings harboring BIL1/BZR1-GFP were grown on 1/2 MS medium supplemented with 1  $\mu$ M Brz for 21 days. The phosphorylation status of BIL1/BZR1 in WT, *bil7-1D*, and *BIL7-RNAi* seedlings treated with 25  $\mu$ M bikinin or DMSO (mock) for 5 min, as determined by immunoblot analysis using an anti-GFP antibody. The signal intensities of phosphorylated and dephosphorylated BIL1/BZR1, indicated by arrowheads, are presented as the percentage relative to phosphorylated BIL1/BZR1 in WT plants subjected to DMSO treatment (upper panel). Relative ratio of dephosphorylated BIL1/BZR1 to phosphorylated BIL1/BZR1 (middle panel). The Ponceau-stained membrane is shown as a loading control (bottom panel). pBIL1: phosphorylated BIL1/BZR1. The full-scan blots are shown in Figure S16.

(D, E) BIL7 promotes hypocotyl elongation in *bil1-1D* plants grown on a medium containing Brz in the dark. Hypocotyl phenotypes (D) and hypocotyl lengths (E) of WT, *bil7-1D*, *bil1-1D*, and *bil7-1D* $\times$ *bil1-1D* seedlings grown on medium supplemented with 3  $\mu$ M Brz in the dark for 7 days (one-way ANOVA followed by Tukey–Kramer test,  $P < 0.05$ ;  $n \geq 32$ ).

suggest that BIL7 is an important factor driving plant growth mechanisms related to BR signaling.

In our study, *Arabidopsis* inflorescence length was increased in *bil7-1D* and *BIL7-OX* plants and decreased in *BIL7-RNAi* plants (Figure 2). Root length was reduced in *BIL7-RNAi* plants. By observing epidermal cells in inflorescences and roots, we found that cell lengths in the *BIL7-RNAi* plants were shorter than those in WT plants. Although the cell length of the inflorescence in *bil7-1D* plants was the same as that in WT plants, the final inflorescence length was greater (Figure 2). This phenotype could result from the elongation of the period before the inflorescence cell terminates its cell division. These results suggest that BIL7 plays important roles in cell elongation and cell division.

Although BIL7 does not contain any previously characterized functional domains, the differential localization of

BIL7 in each cell at variable developmental stages suggests that the subcellular localization of BIL7 plays an important role in cell regulation. We propose models for BIL7 function in BR signaling that show BIL7 relocation from the plasma membrane to the nucleus with three steps (Figure 8). In general, BIL7-GFP is anchored to the plasma membrane in the absence of BL treatment and in fully developed cells. BIL7-GFP is released from the membrane and translocated into nuclei in response to bikinin, which inhibits the negative regulator BIN2, and/or in actively elongating cells. According to general knowledge of the basal side of the root apical meristem, the generation of root cells starts with stem cells surrounding QC cells. In the meristem of the root, the initial cells are actively dividing, and the cell length remains constant. The meristem cells subsequently enter the elongation zone through the transition zone, where cells stop dividing and quickly start to increase in length. In both

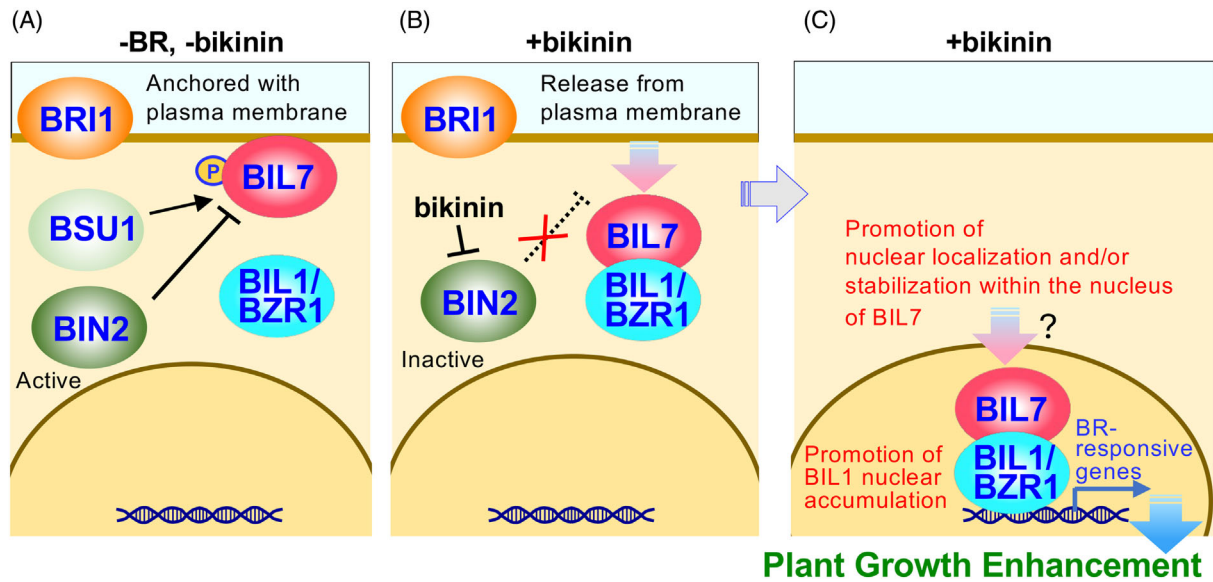


**Figure 8.** A working model of how BIL7 enhances plant growth through regulation of BIL1/BZR1. (A) In the absence of BR, BIN2 phosphorylates BIL7. BIN2-induced phosphorylation of BIL7 controls its extranuclear localization. (B) In the presence of bikinin, inhibition of BIN2 suppresses phosphorylation of BIL7, prompting dissociation of BIL7 from the plasma membrane, thereby facilitating interaction with the transcription factor BIL1/BZR1. (C) BIL7 localizes to the nucleus and/or stabilizes within the nucleus. BIL7 promotes the accumulation of BIL1/BZR1 in the nucleus. High accumulation of BIL1/BZR1 enhances plant growth. P indicates protein phosphorylation.

*BIL7-GFP* plants driven by its native promoter and the 35S promoter, nuclear localization of BIL7 in the transition zone and elongation zone was greater than that in the meristem. Based on sequential protein dynamics, the BIL7-GFP released from the plasma membrane upon activation of BR signaling, which is involved in BIN2 inhibition, might traverse the cytosol and enter the nucleus. Furthermore, nuclear localization of BIL7 plays an important role in the early stage of cell elongation.

We also analyzed the ratio of cells displaying nuclear accumulation of BIL7-GFP, with or without 1  $\mu$ M BL treatment, under a low concentration of 10  $\mu$ M bikinin for 1 h. Under these conditions, a slightly higher ratio of cells showed BIL7 nuclear accumulation in the presence of BL compared to the absence of BL (Figure S15). Although the nuclear accumulation ratio of BIL7-GFP was observed following a single BL treatment, the difference in signal intensity between BL-treated and untreated cells was significantly less pronounced compared to the nuclear accumulation observed after treatment with a high concentration of bikinin.

Bikinin is an inhibitor of the negative kinase BIN2 during BR signaling. BIN2 is known to play an important role not only in BR signaling but also in response to light, other phytohormones, and peptide hormones, as well as other cell dynamics (Nolan et al., 2020; Youn & Kim, 2015). The "*Brz-insensitive-long hypocotyl*" phenotype, the feedback-like downregulation of BR biosynthesis gene expression and the decrease in BR compounds demonstrate that BIL7

is a positive BR signaling component. Nevertheless, these findings for BIL7 localization suggest that BIL7 plays role in several additional signaling pathways regulated by BIN2. Future analyses of the relationship between BIL7 and BR signaling may reveal additional functions of BIL7 and its regulation by signaling pathways.

BIL7 is localized to the cytosol and the nucleus from the plasma membrane. BIL7 also directly interacts with BIL1/BZR1 in the cytosol and nucleus. BIL1/BZR1 is well known as master transcription factors in BR signaling that regulate the expression of BR-related genes (Kim et al., 2009). These possible functions of BIL7 on BIL1/BZR1 might be predicted and considered by the comparison between previous reports and our observations, as depicted in Figure 7. In the root apical meristem, *BIL1/BZR1* native promoter-driven BIL1/BZR1-YFP accumulation in the nucleus was low in the meristematic zone and high in the transition and elongation zones (Chaiwanon & Wang, 2015). The current single-nuclei analysis suggested that the gradient of nuclear accumulation of BIL1/BZR1-YFP from the meristematic zone to the elongation zone is involved in cell type-specific regulation of gene expression (Nolan et al., 2023). We observed that the BIL7 native promoter-driven BIL7-GFP and the 35S promoter-driven GFP-BIL7 also accumulated at higher levels in the cells in the transition zone from the meristem to the elongation zone (Figure 6). Due to the similar expression and nuclear localization of BIL7-GFP and BIL1/BZR1-YFP in the root tip,

a tight relationship between BIL7 and BIL1/BZR1 can be predicted.

The enhanced nuclear accumulation of BIL1/BZR1 by BIL7 may be a consequence of the promotion of stabilization and/or nuclear transport of BIL1/BZR1. The BIL1/BZR1 protein contains a PEST domain that is known to be related to protein degradation. An amino acid mutation was identified in the PEST domain of the *bil1-d/bzr1-1d* mutant that increased dephosphorylation of the *bil1/bzr1* protein and ultimately decreased its degradation by the proteasome (Tang et al., 2011; Wang et al., 2002). BIL7 directly interacted with BIL1/BZR1 (Figure 6), and activated/dephosphorylated BIL1/BZR1 protein accumulation was enhanced in *bil7-1D* (Figure 7). These results suggest that the BIL7 protein stabilizes the activated form of BIL1/BZR1 and/or protects the BIL1/BZR1 protein from degradation.

BIL7 is phosphorylated by BIN2 and dephosphorylated by BSU1. The nuclear localization of BIL7 was enhanced by the BIN2 inhibitor bikinin (Figure 5). Furthermore, BIL7 was found to interact with BIL1/BZR1 in both the cytosol and nucleus. These sequential molecular events surrounding BIL7 suggest that its phosphorylation status may influence the interaction and/or regulation of BIL1/BZR1. Given that the molecular weights of phosphorylated and dephosphorylated forms of BIL1/BZR1 differ significantly, we detected interactions of BIL7 with both phosphorylated and dephosphorylated BIL1/BZR1 (Figure 6). Although phosphorylated BIL7 was identified by Phos-tag SDS-PAGE as a mobility-shifted signal, it remains challenging to determine whether both phosphorylated and dephosphorylated forms of BIL7 can interact with BIL1/BZR1. Further analysis of the biological significance of BIL7's phosphorylation status for BIL1/BZR1 regulation will provide insights into the detailed molecular mechanisms underlying BR signaling in the near future.

The BIL1/BZR1 protein is well known to be imported into the nucleus from the cytoplasm after BR treatment and BR signaling activation (Wang et al., 2002), and nuclear transport of BIL1/BZR1 correlates with dephosphorylation of BIL1/BZR1 (Wang et al., 2021). Although the inhibitory effects of BSS1 and 14-3-3 on the nuclear import of the BIL1/BZR1 protein have been reported (Gampala et al., 2007; Shimada et al., 2015), the factor that promotes the nuclear import of BIL1/BZR1 has not been revealed well. BIL7 interacted with BIL1/BZR1 both in the nucleus and in the cytosol (Figure 6). The nuclear fluorescence signal of BIL1-GFP was greater in *bil7-1D* than in the WT background, and the dephosphorylated BIL1/BZR1 protein signal was greater than the phosphorylated BIL1/BZR1 signal in *bil7-1D* (Figure 7). These results suggest that BIL7 interacts with BIL1/BZR1 in the cytosol and facilitates the nuclear transport of BIL1/BZR1. In animals, the role of the importin family of proteins in transporting proteins to the nucleus from the cytosol has been well documented. An

importin protein homolog has been identified in Arabidopsis. This protein may facilitate protein import to the nucleus and help with environmental adaptation (Merkle, 2011). Although the amino acid sequence of BIL7 is different from that of the Arabidopsis importin family protein homolog, BIL7 might be the long-sought-after nuclear transporter of BIL1/BZR1. Future analysis will reveal the detailed function of BIL7 in the protein stability and/or nuclear transport of BIL1/BZR1.

BIL7 interacted with BIL1/BZR1 but not with BES1 or its homologs BEH1-4, which are homologs of BIL1/BZR1 (Figure S13). While the DNA-binding domains of BIL1/BZR1 and BES1 are highly conserved, their amino acid sequences in other regions show partial differences (Nosaki et al., 2018, 2022). These results suggest that BIL7 may specifically recognize these divergent amino acid regions in BIL1/BZR1.

Since single knockouts of BIL1/BZR1 did not result in significant phenotypic changes (Chen et al., 2019), the reduced interaction between BIL7 and BIL1/BZR1 may not fully explain the semidwarf phenotype observed in *BIL7-RNAi* transgenic plants. To address this question, the discovery that BIL7 has three homologs in Arabidopsis, termed BIL7 homologs (BSHs) (Figure S2A), as well as homologs in many other plant species (Figure S2B,C), may provide valuable insights. Further analysis of various combinations between members of the BIL1/BZR1/BES1 family and the BIL7/BSH family could help clarify the underlying cause of the semidwarf phenotype in *BIL7-RNAi* transformants.

Recent studies have reported possible functional roles of the BIL7 family genes. Plants overexpressing BIL9/BSH2, a homolog of BIL7, exhibited resistance to Brz. Overexpression of BIL9/BSH2 has been demonstrated to enhance drought resistance (Surina et al., 2024). Nevertheless, as BIL9/BSH2 could not interact with BIN2 and BIL1/BZR1, we consider that the detailed molecular function of BIL9/BSH2 in BR signaling is different from that of BIL7 (Surina et al., 2024).

Furthermore, the novel regulators at the plasma membrane (NRPM) 1–4 proteins were identified to be localized on the plasma membrane but not in the nucleus (Xue et al., 2024). In the report, the gene number of NRPM3 is the same as that of BIL7. The authors made triple mutant *nrpm1/2/4* that showed, abnormal patterning of stomata. These findings suggest the multifaceted functions of BIL7 family proteins.

*bil7-1D* inflorescences were longer than *bil1-D/bzr1-1D* inflorescences, which were slightly longer than those of WT. The inflorescence height of *bil7-1D* was also the greatest among all the BR signaling gain-of-function mutants or transformants. The increase in the height by approximately 70% and the increase in the 2nd inflorescence number by approximately 40% of the changes in plant phenotype observed in *bil7-1D* plants seems to lead to an increase in

plant biomass. In contrast, growth inhibition was observed in *BIL7-RNAi* plants (Figure 2A,B). The *nrpm1/2/4* (*bsh1/2/3*) triple mutants showed reduced plant growth, indicating the important role of BIL7 family members in plant growth (Xue et al., 2024). These functions of BIL7 in promoting plant growth and plant biomass production will contribute to the repair of environmental devastation and the improvement of molecular breeding techniques for agriculture in the future.

## EXPERIMENTAL PROCEDURES

### Plant materials and growth conditions

*A. thaliana* ecotype Columbia (Col-0) was used as the wild-type. The *bin2-1*, *det2-1*, *bri1-116*, and *bil1-1D* mutants are in the *A. thaliana* Col-0 background. The *bri1-5* mutant is in the *A. thaliana* Wassilewskija (*Ws-0*) background. The methods used for seed sterilization and the conditions for plant growth have been described previously (Miyaji et al., 2014).

### Screening for the *bil7-1D* mutant

Approximately 8000 RIKEN Arabidopsis FOX hunting lines (Ichikawa et al., 2006) were screened on a 1/2 MS medium containing 3  $\mu$ M Brz (Asami et al., 2000). After 7 days of growth in darkness, seedlings with hypocotyls longer than those of the controls were transferred to soil. Total DNA was extracted from the leaves using a Nucleon Extraction Kit (GE Healthcare, <http://www.gehealthcare.com>). PCR amplification of the FOX fragment was performed using the primers FOX-forward, 5'-GGAAGTTCATTATTCGGA-GAG-3' and FOX-reverse, 5'-GGCAACAGGATTCATCTTAAG-3', followed by sequencing.

### Generating transgenic plants

Full-length *BIL7* CDS with/without a stop codon was amplified from Arabidopsis Col-0 cDNA using the following primers: *BIL7*-forward, 5'-CACCATGAGAAGCGGTGCTAATGG-3' and *BIL7* with stop codon-reverse, 5'-TTAGCTTAGGTACCTGACTG-3', or *BIL7* without stop codon-reverse, 5'-GCTTAGGTACCTGACTGCA-3', and cloned into pENTR/D-TOPO (Invitrogen). To replicate the *bil7-1D* phenotype and knock down *BIL7* expression using RNAi, pENTR-full-length *BIL7* was cloned into the binary vector (Nakagawa, Kurose, et al., 2007) pGWB2 containing a 35S promoter and pGWB80. To observe the subcellular localization of *BIL7* driven by the 35S promoter, pENTR-*BIL7* without a stop codon was cloned into the binary vector pGWB5 containing the 35S promoter and C-terminal GFP, and pENTR-full-length *BIL7* was cloned into the pGWB6 binary vector containing the 35S promoter and N-terminal GFP. To observe the subcellular localization of *BIL7* driven by the *BIL7* promoter, a 2000-bp genomic fragment spanning the *BIL7* promoter region was amplified from Col-0 genomic DNA using *BIL7*-own GFP-forward (5'-CACCTTGCTTCTTTTAAGACTTGT TAGGAAAATACTAAAT-3') and *BIL7* without stop codon-reverse primers and was subsequently cloned into the binary vector (Nakagawa, Suzuki, et al., 2007) pGWB550 containing the GFP sequence but no promoter.

*bil7-1* mutant was generated using the CRISPR-Cas9 system. A guide RNA (5'-AGAGAAAATGGTGAATCGA-3') was designed using CRISPR direct (<https://crispr.dbcls.jp/>). gRNA validity was confirmed by the Guide-it sgRNA *In Vitro* Transcription and

Screening System (Takara, Shiga, Japan). The oligonucleotide for gRNA was cloned into the AarI site of pKIR1.1 (Tsutsui & Higashiyama, 2017). Mutated lines were selected by Sanger sequencing, and null segregants of the CRISPR-Cas9 transgene were used.

To observe *BIL7* expression in various plant organs, a 968-bp genomic fragment spanning the *BIL7* promoter and first exon was amplified from Col-0 genomic DNA using *BIL7*-GUS-forward (5'-CACCGAACCAAGAATCAGTCAATTGCA-3') and *BIL7*-GUS-reverse (5'-ATGAATCGGAGAAGATTGATGA-3') primers and subsequently cloned into the binary vector pGWB3 containing the GUS coding sequence. The inserts were cloned into binary vectors via Gateway (Invitrogen) cloning. These constructs were transformed into Col-0 via the floral dip method (Clough & Bent, 1998).

35S:*BIL1/BZR1-GFP*×*bil7-1D* and 35S:*BIL1/BZR1-GFP*×*BIL7-RNAi-1* were made by crossing each transformant and mutant, not by additional transformation of the 35S:*BIL7-GFP* or 35S:*BIL1/BZR1-GFP* vector to mutants.

### Phylogenetic analysis

Sequences of *BIL7* homologous genes from other plant species were obtained from Phytozome (<https://phytozome-next.jgi.doe.gov/>) and MarpolBase (<https://marchantia.info/>). The amino acid sequences of these *BIL7* homologs were aligned using MAFFT with the G-INS-i algorithm (Kato et al., 2019). Subsequently, a phylogenetic tree was constructed from the alignment data using IQ-TREE (Trifinopoulos et al., 2016). The resulting treefile was visualized and refined using iTOL (Letunic & Bork, 2021). Multiple sequence alignment results were visualized using Genetyx-Mac version 20.1.1.

### Measurement of cell length and number

Ten cells were selected from the fifth internode (from the bottom) of the primary inflorescence of each 91-day-old plant. Internodes from wild-type, *bil7-1D*, and *BIL7-RNAi-1* plants were stained overnight with 20  $\mu$ g mL<sup>-1</sup> PI in 70% [v/v] ethanol, and the stained epidermal cells were imaged using a confocal laser-scanning microscope (Zeiss). The cell length in each stained internode was measured using six plants per line with ImageJ software (<http://rbs.info.nih.gov/ij/>). The cell number was calculated by dividing the internode length by the average cell length. The experiment was repeated at least twice with similar results.

### qRT-PCR

Arabidopsis plants or suspension cells were ground in liquid nitrogen, and total RNA was extracted with an RNeasy Plant Mini Kit (Qiagen, Hilden, Germany) using an RLT and RLC buffer, respectively. The methods for cDNA synthesis and qRT-PCR have been described previously (Miyaji et al., 2014). The following primers were used for qRT-PCR: *DWF4*, 5'-CATAAAGCTCTCTTCAGT CACGA-3' and 5'-CGTCTGTTCTTTGTTTCTAA-3'; *CPD*, 5'-CACTT CAAAGATGCTCGCACTT-3' and 5'-CAGCTCGTAACCGGGACATAG-3'; *BIL7*, 5'-CATTCGTCTCTCGGGTCCA-3' and 5'-TCTTCGGCGAAG CTGATCTA-3'; *BIL7-RNAi*, 5'-CGAGAAAATCTCAGACTCA-3' and 5'-AAGCAGCTGCGTTTATAGTA-3'; *BSH1*, 5'-CGGATCGAAACAG AGGAGAGT-3' and 5'-CAGCATCCATGTTCAAGGTTTG-3'; *BSH2*, 5'-AGCGGCGAACATTTAAGACCAA-3' and 5'-GCTTCCCATGTTAG AGGTAATGAAG-3'; *BSH3*, 5'-CTCTGATGCAGAGGTCGAGTAC-3' and 5'-CACTTTCTCACCTTGCTCTCT-3'; *eIF4a*, 5'-TGACCACACAG TCTCTGCAA-3' and 5'-ACCAGGGAGACTTGTTGGAC-3'; *cEYFP*, 5'-GCTGCTGCCGACAACC-3' and 5'-GTCCATGCCGAGAGTGATCC-3'; and *nEYFP*, 5'-GACGTAACGGCCACAAGTT-3' and 5'-CGTAG CCCGAAGGTGGTCAC-3'.

## BR measurements

Approximately 10 g (fresh weight) of tissue from the aerial parts of 6-week-old plants was extracted using 500 mL of MeOH, followed by the addition of deuterium-labeled internal standards. BR purification and quantification were performed as described previously (Fujioka et al., 2002).

## GUS staining

GUS histochemical staining was performed as described previously (Shimada et al., 2015). Digital images were captured using an Olympus SZX16 microscope (Olympus, Tokyo, Japan).

## Confocal laser-scanning microscopy

The *35S:BIL7-GFP*, *BIL7pro:BIL7-GFP*, and *35S:BIL1/BZR1-GFP* plants were observed using a LSM700 (Zeiss, Jena, Germany) and SP8 Falcon (Leica Microsystems, Wetzlar, Germany). To observe the nuclear localizations of BIL7, plants were grown on the medium containing 1.5% (w/v) sucrose for 3 days. The plants were stained with 1  $\mu\text{g mL}^{-1}$  DAPI for 10 min at room temperature.

## Nuclear fractionation

*35S:BIL7-GFP* plants (1 g) were harvested and ground to a fine powder in liquid nitrogen and mixed with 2 mL  $\text{g}^{-1}$  of lysis buffer (20 mM Tris-HCl, pH 7.5, 20 mM KCl, 2 mM EDTA, 2.5 mM  $\text{MgCl}_2$ , 25% glycerol, 250 mM Suc, and 1 mM DTT) supplemented with protease inhibitor cocktail (Roche, Basel, Switzerland). The homogenate was filtered through a double layer of Miracloth, and the flow-through fraction was used as total protein. The flow-through was spun at 1500 $\times g$  for 10 min at 4°C. The pellet was washed three times with 3 mL of nuclear resuspension buffer NRB1 (20 mM Tris-HCl, pH 7.4, 25% glycerol, 2.5 mM  $\text{MgCl}_2$ , and 0.2% Triton X-100) and then resuspended with 3 mL of NRB (20 mM Tris-HCl, pH 7.4, 25% glycerol, and 2.5 mM  $\text{MgCl}_2$ ). The final nuclear pellet was resuspended in 200  $\mu\text{L}$  1 $\times$  SDS sample buffer. The protein content was quantified using a Bio-Rad protein assay kit. As quality controls for the fractionation, histone H3 (Abcam, Cambridge, UK) was probed and used as nuclear markers.

## Microsomal fractionation

Four-day-old *35S:BIL7-GFP* plants (1 g) were harvested and ground to a fine powder in liquid nitrogen and mixed with 4 mL  $\text{g}^{-1}$  of lysis buffer (250 mM Tris-HCl, pH 8, 25 mM EDTA, 290 mM Suc, and 3 mM DTT) supplemented with protease inhibitor cocktail (Roche). The homogenate was filtered through a double layer of Miracloth, and the flow-through fraction was used as total protein. The flow-through was spun at 10 000 $\times g$  for 10 min at 4°C. The supernatant was centrifuged at 150 000 $\times g$  for 45 min at 4°C. The pellet was resuspended in 50  $\mu\text{L}$  1 $\times$  LDS sample loading buffer (3% LDS, 60 mM Tris-HCl pH 6.8, 60 mM LDS, 6% [w/v] sucrose, and 0.003% [w/v] BPB). The protein content was quantified using a Bio-Rad protein assay kit. As quality controls for the fractionation,  $\text{H}^+\text{ATPase}$  (Agrisera, Vännäs, Sweden) was probed and used as plasma membrane markers.

## Assay of the translocation of GFP-BIL7 between the plasma membrane and the nucleus

Fluorescence images of cells in the root transition zone were obtained and scanned along a line drawn on the cell including the nucleus and plasma membrane. From the resulting intensity

profiles, the average peak pixel intensity at the two cell boundaries (plasma membrane) and the average pixel intensity inside the nucleus (nucleus) were obtained.

## Yeast two-hybrid analysis

The CDS encoding BIL1/BZR1 without the first 21 amino acids (He et al., 2002), BES1 without the first 20 amino acids (He et al., 2002), BRI1 without the first 814 amino acids (Li & Chory, 1997), BAK1 without the first 249 amino acids (Li et al., 2002; Nam & Li, 2002), full-length BIL7, BIN2, BSU1, BK11 (Wang & Chory, 2006), BSK1 (Tang et al., 2008), CDG1 (Kim et al., 2011), 14-3-3 $\lambda$ , 14-3-3 $\kappa$ , PP2A-B- $\alpha$  (Tang et al., 2011; Wang et al., 2016; Wu et al., 2011), PP2A-B- $\beta$  (Tang et al., 2011; Wang et al., 2016; Wu et al., 2011), BIL7 $\Delta$ C1 (1–316 aa), BIL7 $\Delta$ C2 (1–256 aa), and BIL7C (257–358 aa), and mutant *bil1-1D/bzr1-1D* (P234L) (Wang et al., 2002) were cloned into pENTR/D-TOPO (Invitrogen) and subsequently cloned into the pDEST22 (Invitrogen) prey vector or pDEST32 (Invitrogen) bait vector. The plasmids used for the interaction analysis of BIL7 with BIN2, BSU1, BIL1/BZR1, BES1, PP2A-B- $\alpha$ , and PP2A-B- $\beta$  were transformed into yeast strain Y2HGold (Clontech), and the other plasmids were transformed into yeast strain AH109 (Clontech). Each analysis was performed using at least three different yeast colonies.

## BiFC

The full-length *BIL7*, *BIN2*, *BSU1*, *BIL1/BZR1*, and *BRI1* CDS without a stop codon were cloned into pENTR/D-TOPO (Invitrogen) and were subsequently cloned into the pB4GWnY or pB4GWcY (Kamigaki et al., 2016) vector via LR recombination. The Arabidopsis suspension culture line Alex was transformed as described previously (Saito et al., 2011). Four days after *Agrobacterium* inoculation, fluorescence was detected using an LSM700 microscope (Zeiss, Jena, Germany).

## Transient expression in *N. benthamiana*

Transient expression assays in *N. benthamiana* were performed as previously described (Kondo et al., 2014). Full-length *BIL7*, *BSU1*, and *BIL1/BZR1* CDS without a stop codon were cloned into pENTR/D-TOPO (Invitrogen) and were subsequently cloned into pGWB5 or pGWB520 containing the *35S* promoter and 10 $\times$  Myc via LR recombination. Leaf samples were harvested for protein extraction approximately 36 h after infiltration.

## Coimmunoprecipitation analysis

To analyze the interaction of BIL7 with BIN2 or BIL1/BZR1, total proteins were extracted from 4 to 6 g of *N. benthamiana* leaf tissue by grinding in liquid nitrogen, followed by further grinding in 1.3 volumes of a cold extraction buffer (50 mM Tris-HCl, pH 7.5, 150 mM NaCl, 5 mM EDTA, 0.1% [v/v] Triton X-100, 0.2% [v/v] Nonidet P-40, 10  $\mu\text{M}$  MG132, 1 mM phenylmethylsulfonyl fluoride (PMSF), and protease inhibitor cocktail [Roche Diagnostics]). The extract was centrifuged at 20 000 $\times g$  for 30 min at 4°C. The supernatant was incubated for 1.5 h at 4°C with 50  $\mu\text{L}$  of anti-c-Myc agarose (Sigma-Aldrich, St Louis, MO, USA, A7470). The beads were collected and washed four times with the cold extraction buffer and eluted with 70  $\mu\text{L}$  of a 2 $\times$  LDS sample loading buffer.

To analyze the interaction of BIL7 with BIN2 in Arabidopsis, total proteins were extracted from 250 mg of 7-day-old Arabidopsis seedlings by grinding in liquid nitrogen, followed by further grinding in 4 volumes of a cold extraction buffer (50 mM Tris-HCl, pH 7.5, 150 mM NaCl, 5 mM EDTA, 0.1% [v/v] Triton X-100, 0.2% [v/v] Nonidet P-40, 1 mM PMSF, and protease inhibitor cocktail

[Roche Diagnostics]). The extract was centrifuged at 12 000 rpm for 5 min at 4°C. The supernatant was incubated for 30 min at 4°C with 30 µL of GFP-trap agarose beads (ChromoTek, Munich, Germany). The beads were collected and washed four times with the cold extraction buffer and eluted with 80 µL of a 2× SDS sample loading buffer.

To analyze the interaction of BIL7 with BSU1 or BIL1/BZR1, total proteins were extracted from 200 mg of *N. benthamiana* leaf tissue by grinding in liquid nitrogen, followed by further grinding in 600 µL of a cold resuspension buffer containing 10 µM MG132. The extract was centrifuged at 20 000×g for 30 min at 4°C. The supernatant was incubated for 1 h at 4°C with 50 µL of anti-GFP magnetic beads (Miltenyi Biotec, Bergisch Gladbach, Germany). The magnetic beads were washed, and the bound proteins were eluted with 120 µL of elution buffer (Miltenyi Biotec) preheated at 95°C. The composition of the resuspension and rinsing buffers and the method used to wash the magnetic beads have been described previously (Fabregas et al., 2013). After incubation at 100°C for 5 min, the proteins were detected via immunoblot analysis using monoclonal anti-HA antibody 3F10 (Roche Diagnostics) at a 1:3000 dilution, polyclonal anti-GFP antibody (Molecular Probes, Carlsbad, CA, USA) at a 1:7500 dilution, and monoclonal anti-Myc antibody 9E10 (Sigma-Aldrich) at a 1:35 000 dilution in Western blot Immuno Booster Solution 1 (Takara). The blots were developed using horseradish peroxidase-linked secondary antibodies in Western blot Immuno Booster Solution 2 (Takara) and the Immobilon Western Chemiluminescent substrate (Millipore). As a negative control, leaves were infiltrated with *Agrobacterium* without the vector (control). To analyze the interaction of BIL7 with BSU1, leaves were infiltrated with 100 nM BL 1 h before harvesting. Each Co-IP experiment was repeated at least three times with similar results.

### ***In vitro* kinase assay**

For the *in vitro* kinase assays, the codon-optimized Arabidopsis BIL1/BZR1 (21–336) gene was cloned into the expression vector pMAL-c2X (New England Biolabs, Ipswich, MA, USA) and subsequently transformed into the *E. coli* strain BL21(DE3) (Novagen, Madison, WI, USA). The CDS fragments of the full-length Arabidopsis BIL7 sequence (1–358) were also cloned into the pMAL-c2X vector and subsequently transformed into the *E. coli* strain Rosetta(DE3) (Novagen). Protein expression was induced by isopropyl β-D-1-thiogalactopyranoside (IPTG) treatment for 2 h at 37°C. The expressed proteins contained a maltose-binding protein (MBP) tag at their N-terminus.

For purification, the cell pellets were lysed by sonication, and the soluble fractions were separated by centrifugation and loaded onto an amylose resin (New England Biolabs) with buffer A (20 mM Tris-HCl, pH 7.5, 1 M NaCl, 0.5 mM EDTA, 1 mM DTT, and 10% [v/v] glycerol). After the fusion proteins were washed with buffer A, they were eluted with buffer B (20 mM Tris-HCl, pH 7.5, 1 M NaCl, 0.5 mM EDTA, 1 mM DTT, 20 mM maltose, and 10% [v/v] glycerol). The eluates were concentrated and run over a Superdex 200 10/300 GL column (Cytiva) with buffer C (20 mM Tris-HCl, pH 7.5, 500 mM NaCl, 1 mM DTT, and 10% [v/v] glycerol).

The CDS fragments of Arabidopsis full-length BIN2 (1–382) were cloned into the pGEX-6P-3 vector (Cytiva) and subsequently transformed into *E. coli* Rosetta(DE3) cells. Protein expression was induced by IPTG treatment for 16 h at 18°C.

For purification, the cell pellets were lysed by sonication in buffer D (20 mM Tris-HCl, pH 8.0, 300 mM NaCl, 1 mM DTT, and 5% glycerol). The supernatant was loaded onto a disposable polypropylene column packed with a glutathione Sepharose 4B resin

(Cytiva), and the column was washed with buffer D. On-column cleavage was performed overnight at 5°C by adding HRV3C protease, and the target protein was eluted. BIN2 was further purified using a Mono Q column (Cytiva) and was eluted from the column using a 0–500 mM NaCl gradient in 20 mM Tris-HCl, pH 8.0, 1 mM DTT, and 5% [v/v] glycerol.

*In vitro* kinase reactions were performed using 2.5 µM BIN2 and 2.5 µM of each MBP-fusion protein in buffer E (20 mM MOPS-KOH, pH 7.5, 300 mM KCl, 5 mM ATP, 5 mM MgCl<sub>2</sub>, 5 mM DTT, and 10% [v/v] glycerol). The reaction was incubated at 5°C for 16 h and terminated by adding 2× sample buffer for SDS-PAGE and boiling for 5 min. The proteins were separated by SDS-PAGE. After electrophoresis, the gel was stained using a Pro-Q Diamond phosphoprotein gel stain (Invitrogen), followed by a SYPRO Ruby protein gel stain (Invitrogen). The staining procedures were carried out according to the manufacturer's instructions. Fluorescence was detected using a LAS4000 system (Cytiva).

### **Detection of *in vivo* BIL7 phosphorylation**

The *in vivo* phosphorylation status of BIL7 was analyzed using Phos-tag biotin (Wako, Osaka, Japan). Plant materials were ground in liquid nitrogen and resuspended in IP buffer (50 mM Tris pH 7.5, 150 mM NaCl, 2 mM EDTA, 1% [v/v] Nonidet P-40, 0.5% [w/v] sodium deoxycholate, 1 mM PMSF, protease inhibitor cocktail, and phosphatase inhibitor [Roche]). The protein extracts were incubated with GFP-trap beads (Chromotek) at 4°C for 0.5 h. The beads were washed three times with washing buffer (50 mM Tris pH 7.5, 150 mM NaCl, 1 mM PMSF, and EDTA-free protease inhibitor cocktail), and the phosphorylation level of immunopurified BIL7 was determined by blotting with Phos-tag biotin.

The *in vivo* phosphorylation status of BIL7 was analyzed using CIP. Proteins were extracted from *N. benthamiana* leaf tissue with extraction buffer (50 mM Tris-HCl, pH 7.5, 150 mM NaCl, 3% [v/v] Nonidet P-40, 1.5% [w/v] sodium deoxycholate, 1 mM PMSF, and protease inhibitor cocktail [Roche Diagnostics]) and then incubated with CIP (Takara) at 37°C for 1 h and subsequently separated on a 6% SDS-PAGE gel containing 50 µM Phos-tag (Wako). The separated proteins were then transferred to a PVDF membrane (Cytiva) and blotted with an anti-GFP antibody (1:20 000) in Western blot Immuno Booster Solution 1. The secondary antibody was anti-rabbit-HRP (1:40 000, Promega) in Western blot Immuno Booster Solution 2.

### **Immunoblot analysis**

To analyze the phosphorylation status of BIL1/BZR1, total proteins were extracted from light-grown 21-day-old seedlings using a 1× SDS sample buffer and detected by immunoblot analysis using a polyclonal antibody against GFP. Protein extraction and immunoblotting were performed as described previously (Shimada et al., 2015). The immunoblot analyses of BIL7, BIN2, and BSU1 were performed with *N. benthamiana* extracts infiltrated with *Agrobacterium* carrying BIL7-GFP (pGWB5-BIL7) and/or BIN2-HA or BSU1-HA (both cloned into pK7m34GW).

### **Assay of the translocation of BIL1-GFP between the cytosol and nucleus**

The transgenic lines were crossed with plants expressing a 35S: BIL1/BZR1-GFP. F1 plants were grown on a medium containing 1 µM Brz in darkness for 4 days. Fluorescence images of cells in the root transition zone were obtained and scanned along a line drawn in the nucleus. From the resulting intensity profiles, the average pixel intensity inside the nucleus (nucleus) was obtained.

### In vitro pull-down assay

The CDS encoding BIL1/BZR1 and its homologs (BES1, BEH1, BEH2, BEH3, and BEH4) were cloned into the pMAL-c6T vector (New England Biolabs), and the CDS encoding BIL7 was cloned into the pH6HTN His6HaloTag T7 vector (Promega). Linearized template DNA was amplified from each expression vector and used for protein expression with PUREfrex 2.0 (GeneFrontier) and EF-P (GeneFrontier) in a total volume of 10  $\mu$ L, following the manufacturer's instructions. For the pull-down assay, reaction solutions containing HaloTag-BIL7 and each of MBP-BIL1/BZR1 homologs were mixed with Amylose magnetic beads (New England Biolabs) in 100  $\mu$ L of the binding buffer (phosphate-buffered saline (PBS) with 500 mM NaCl and 0.005% Nonidet P-40) for 1 h at 4°C. The resin was washed three times with 1 mL of binding buffer. The bound proteins were eluted by incubating the resin in an LDS sample buffer for 30 min at 25°C and then analyzed using SDS-PAGE, followed by Western blotting. HaloTag-BIL7 was detected using an anti-HaloTag antibody (Promega), while MBP-fusion proteins were detected with an anti-MBP antibody (New England Biolabs).

### AUTHOR CONTRIBUTIONS

TN designed the research; ToM, AY, YN, SF, SN, and TaM performed the research; KN, RT, SM-G, MT, MM, HO, KS, and TA analyzed the data; and TN, ToM, and AY wrote the paper.

### ACKNOWLEDGMENTS

We are deeply saddened by the recent passing away of Dr. Joanne Chory, whose great works for BR biosynthesis, perception, and signaling research provided the basis for many of our studies. We also wish to thank Dr. Joanne Chory for her fruitful discussions about the research of our BR research, including BIL7. We wish to thank T. Nakagawa for providing the pGWB cloning vectors, S. Mano for providing the BiFC binary vectors, Y. Kondo, C. Saito, and H. Fukuda for technical advice and the Arabidopsis suspension cell cultures, and K. Saeki for technical assistance with the BiFC assay. This work was supported by Kyoto University Live Imaging Center. This work was supported in part by grants from the NARO Bio-oriented Technology Research Advancement Institution (BRAIN) to TN and TA, a grant from CREST, Japan Science and Technology Agency to TN and TA, and a grant from JSPS KAKENHI (Grant Numbers: JP18H02140 to TN; JP24H00502 to TN, TaM, and AY; and JP21H02114 to TN, TaM, and SN).

### CONFLICT OF INTEREST STATEMENT

The authors declare no conflict of interest.

### DATA AVAILABILITY STATEMENT

All relevant data are included in this manuscript and its supporting information. Further inquiries or requests for materials can be directed to [nakano.takeshi.6x@kyoto-u.ac.jp](mailto:nakano.takeshi.6x@kyoto-u.ac.jp).

### SUPPORTING INFORMATION

Additional Supporting Information may be found in the online version of this article.

**Figure S1.** Gene expression analysis of *BIL7* and sensitivity analysis to Brz in *BIL7-OX* plants.

**Figure S2.** The Arabidopsis BIL7 amino acid sequence is conserved among diverse plant species.

**Figure S3.** *bil7-1* was less sensitive to BL compared to the wild-type.

**Figure S4.** Phenotypes and *BIL7* gene expression in *bil7-1D*, *BIL7-OX1*, *BIL7-OX2*, and *BIL7-RNAi-1* plants.

**Figure S5.** *BIL7* gene expression was detected in developing tissues of wild-type plants.

**Figure S6.** BIL7-GFP and GFP-BIL7 are functional.

**Figure S7.** Subcellular localization of BIL7-GFP in *35S:BIL7-GFP* plant.

**Figure S8.** Hydrophobicity plot of BIL7.

**Figure S9.** *bil7-1D* partially suppresses the *det2-1* and *bri1-5* phenotypes.

**Figure S10.** BIL7 does not interact with BRI1, BAK1, BK1, BSK1, CDG1, 14-3-3 $\lambda$ a, 14-3-3 $\kappa$ , PP2A-B- $\alpha$ , or PP2A-B- $\beta$ .

**Figure S11.** Expression of transcripts from BiFC vectors.

**Figure S12.** Nuclear localization of BIL7 in the root transition zone.

**Figure S13.** BIL7 interacts with BIL1/BZR1 but not BES1.

**Figure S14.** BIL7 and BIL1/BZR1 function interdependently in promoting hypocotyl elongation.

**Figure S15.** Full-scan blots.

### REFERENCES

- Alexandersson, E., Saalbach, G., Larsson, C. & Kjellbom, P. (2004) Arabidopsis plasma membrane proteomics identifies components of transport, signal transduction and membrane trafficking. *Plant & Cell Physiology*, **45**, 1543–1556.
- Asami, T., Min, Y.K., Nagata, N., Yamagishi, K., Takatsuto, S., Fujioka, S. *et al.* (2000) Characterization of brassinazole, a triazole-type brassinosteroid biosynthesis inhibitor. *Plant Physiology*, **123**, 93–100.
- Asami, T., Nakano, T., Nakashita, H., Sekimata, K., Shimada, Y. & Yoshida, S. (2003) The influence of chemical genetics on plant science: shedding light on functions and mechanism of action of brassinosteroids using biosynthesis inhibitors. *Journal of Plant Growth Regulation*, **22**, 336–349.
- Asami, T. & Yoshida, S. (1999) Brassinosteroid biosynthesis inhibitors. *Trends in Plant Science*, **4**, 348–353.
- Beemster, G.T., Fiorani, F. & Inzé, D. (2003) Cell cycle: the key to plant growth control? *Trends in Plant Science*, **8**, 154–158.
- Chaiwanon, J. & Wang, Z.Y. (2015) Spatiotemporal brassinosteroid signaling and antagonism with auxin pattern stem cell dynamics in Arabidopsis roots. *Current Biology*, **25**, 1031–1042.
- Chen, L.G., Gao, Z., Zhao, Z., Liu, X., Li, Y., Zhang, Y. *et al.* (2019) BZR1 family transcription factors function redundantly and indispensably in BR signaling but exhibit BRI1-independent function in regulating anther development in Arabidopsis. *Molecular Plant*, **12**, 1408–1415.
- Choe, S., Fujioka, S., Noguchi, T., Takatsuto, S., Yoshida, S. & Feldmann, K.A. (2001) Overexpression of DWARF4 in the brassinosteroid biosynthetic pathway results in increased vegetative growth and seed yield in Arabidopsis. *Plant Journal*, **26**, 573–582.
- Clough, S.J. & Bent, A.F. (1998) Floral dip: a simplified method for Agrobacterium-mediated transformation of *Arabidopsis thaliana*. *Plant Journal*, **16**, 735–743.
- Clouse, S.D., Langford, M. & McMorris, T.C. (1996) A brassinosteroid-insensitive mutant in *Arabidopsis thaliana* exhibits multiple defects in growth and development. *Plant Physiology*, **111**, 671–678.
- de Rybel, B., Audenaert, D., Vert, G., Rozhon, W., Mayerhofer, J., Peelman, F. *et al.* (2009) Chemical inhibition of a subset of *Arabidopsis thaliana* GSK3-like kinases activates brassinosteroid signaling. *Chemistry & Biology*, **16**, 594–604.
- Fabregas, N., Li, N., Boeren, S., Nash, T.E., Goshe, M.B., Clouse, S.D. *et al.* (2013) The brassinosteroid insensitive1-like3 signalosome complex regulates Arabidopsis root development. *Plant Cell*, **25**, 3377–3388.
- Fujioka, S., Takatsuto, S. & Yoshida, S. (2002) An early C-22 oxidation branch in the brassinosteroid biosynthetic pathway. *Plant Physiology*, **130**, 930–939.

- Gampala, S.S., Kim, T.W., He, J.X., Tang, W., Deng, Z., Bai, M.Y. *et al.* (2007) An essential role for 14-3-3 proteins in brassinosteroid signal transduction in Arabidopsis. *Developmental Cell*, **13**, 177–189.
- Gonzalez-Garcia, M.P., Vilarrasa-Blasi, J., Zhiponova, M., Divol, F., Mora-Garcia, S., Russinova, E. *et al.* (2011) Brassinosteroids control meristem size by promoting cell cycle progression in Arabidopsis roots. *Development*, **138**, 849–859.
- Guo, H., Li, L., Aluru, M., Aluru, S. & Yin, Y. (2013) Mechanisms and networks for brassinosteroid regulated gene expression. *Current Opinion in Plant Biology*, **16**, 545–553.
- He, J.X., Gendron, J.M., Sun, Y., Gampala, S.S., Gendron, N., Sun, C.O. *et al.* (2005) BZR1 is a transcriptional repressor with dual roles in brassinosteroid homeostasis and growth responses. *Science*, **307**, 1634–1638.
- He, J.X., Gendron, J.M., Yang, Y., Li, J. & Wang, Z.Y. (2002) The GSK3-like kinase BIN2 phosphorylates and destabilizes BZR1, a positive regulator of the brassinosteroid signaling pathway in Arabidopsis. *Proceedings of the National Academy of Sciences of the United States of America*, **99**, 10185–10190.
- Ichikawa, T., Nakazawa, M., Kawashima, M., Iizumi, H., Kuroda, H., Kondou, Y. *et al.* (2006) The FOX hunting system: an alternative gain-of-function gene hunting technique. *Plant Journal*, **48**, 974–985.
- Kamigaki, A., Nito, K., Hikino, K., Goto-Yamada, S., Nishimura, M., Nakagawa, T. *et al.* (2016) Gateway vectors for simultaneous detection of multiple protein–protein interactions in plant cells using bimolecular fluorescence complementation. *PLoS One*, **11**, e0160717.
- Katoh, K., Rozewicki, J. & Yamada, K.D. (2019) MAFFT online service: multiple sequence alignment, interactive sequence choice and visualization. *Briefings in Bioinformatics*, **20**, 1160–1166.
- Kim, T.W., Guan, S., Burlingame, A.L. & Wang, Z.Y. (2011) The CDG1 kinase mediates brassinosteroid signal transduction from BRI1 receptor kinase to BSU1 phosphatase and GSK3-like kinase BIN2. *Molecular Cell*, **43**, 561–571.
- Kim, T.W., Guan, S., Sun, Y., Deng, Z., Tang, W., Shang, J.X. *et al.* (2009) Brassinosteroid signal transduction from cell-surface receptor kinases to nuclear transcription factors. *Nature Cell Biology*, **11**, 1254–1260.
- Kinoshita, T., Cano-Delgado, A., Seto, H., Hiranuma, S., Fujioka, S., Yoshida, S. *et al.* (2005) Binding of brassinosteroids to the extracellular domain of plant receptor kinase BRI1. *Nature*, **433**, 167–171.
- Kondo, Y., Ito, T., Nakagami, H., Hirakawa, Y., Saito, M., Tamaki, T. *et al.* (2014) Plant GSK3 proteins regulate xylem cell differentiation downstream of TDIF-TDR signalling. *Nature Communications*, **5**, 3504.
- Leticun, I. & Bork, P. (2021) Interactive Tree Of Life (iTOL) v5: an online tool for phylogenetic tree display and annotation. *Nucleic Acids Research*, **49**, W293–w296.
- Li, J. & Chory, J. (1997) A putative leucine-rich repeat receptor kinase involved in brassinosteroid signal transduction. *Cell*, **90**, 929–938.
- Li, J., Nagpal, P., Vitart, V., McMorris, T.C. & Chory, J. (1996) A role for brassinosteroids in light-dependent development of Arabidopsis. *Science*, **272**, 398–401.
- Li, J. & Nam, K.H. (2002) Regulation of brassinosteroid signaling by a GSK3/SHAGGY-like kinase. *Science*, **295**, 1299–1301.
- Li, J., Wen, J., Lease, K.A., Doke, J.T., Tax, F.E. & Walker, J.C. (2002) BAK1, an Arabidopsis LRR receptor-like protein kinase, interacts with BRI1 and modulates brassinosteroid signaling. *Cell*, **110**, 213–222.
- Li, Z., Fu, Y., Wang, Y. & Liang, J. (2023) Scaffold protein RACK1 regulates BR signaling by modulating the nuclear localization of BZR1. *New Phytologist*, **239**, 1804–1818.
- Merkle, T. (2011) Nucleo-cytoplasmic transport of proteins and RNA in plants. *Plant Cell Reports*, **30**, 153–176.
- Mitra, S.K., Gantt, J.A., Ruby, J.F., Clouse, S.D. & Goshe, M.B. (2007) Membrane proteomic analysis of *Arabidopsis thaliana* using alternative solubilization techniques. *Journal of Proteome Research*, **6**, 1933–1950.
- Miyaji, T., Yamagami, A., Kume, N., Sakuta, M., Osada, H., Asami, T. *et al.* (2014) Brassinosteroid-related transcription factor BIL1/BZR1 increases plant resistance to insect feeding. *Bioscience, Biotechnology, and Biochemistry*, **78**, 960–968.
- Mora-Garcia, S., Vert, G., Yin, Y., Cano-Delgado, A., Cheong, H. & Chory, J. (2004) Nuclear protein phosphatases with Kelch-repeat domains modulate the response to brassinosteroids in Arabidopsis. *Genes & Development*, **18**, 448–460.
- Nakagawa, T., Kurose, T., Hino, T., Tanaka, K., Kawamukai, M., Niwa, Y. *et al.* (2007) Development of series of gateway binary vectors, pGWBs, for realizing efficient construction of fusion genes for plant transformation. *Journal of Bioscience and Bioengineering*, **104**, 34–41.
- Nakagawa, T., Suzuki, T., Murata, S., Nakamura, S., Hino, T., Maeo, K. *et al.* (2007) Improved gateway binary vectors: high-performance vectors for creation of fusion constructs in transgenic analysis of plants. *Bioscience, Biotechnology, and Biochemistry*, **71**, 2095–2100.
- Nam, K.H. & Li, J. (2002) BRI1/BAK1, a receptor kinase pair mediating brassinosteroid signaling. *Cell*, **110**, 203–212.
- Nolan, T.M., Vukasinović, N., Hsu, C.W., Zhang, J., Vanhoutte, I., Shahan, R. *et al.* (2023) Brassinosteroid gene regulatory networks at cellular resolution in the Arabidopsis root. *Science*, **379**, eadf4721.
- Nolan, T.M., Vukasinović, N., Liu, D., Russinova, E. & Yin, Y. (2020) Brassinosteroids: multidimensional regulators of plant growth, development, and stress responses. *Plant Cell*, **32**, 295–318.
- Nosaki, S., Mitsuda, N., Sakamoto, S., Kusabayashi, K., Yamagami, A., Xu, Y. *et al.* (2022) Brassinosteroid-induced gene repression requires specific and tight promoter binding of BIL1/BZR1 via DNA shape readout. *Nature Plants*, **8**, 1440–1452.
- Nosaki, S., Miyakawa, T., Xu, Y., Nakamura, A., Hirabayashi, K., Asami, T. *et al.* (2018) Structural basis for brassinosteroid response by BIL1/BZR1. *Nature Plants*, **4**, 771–776.
- Ryu, H., Kim, K., Cho, H., Park, J., Choe, S. & Hwang, I. (2007) Nucleo-cytoplasmic shuttling of BZR1 mediated by phosphorylation is essential in Arabidopsis brassinosteroid signaling. *Plant Cell*, **19**, 2749–2762.
- Saito, C., Uemura, T., Awai, C., Tominaga, M., Ebine, K., Ito, J. *et al.* (2011) The occurrence of ‘bulbs’, a complex configuration of the vacuolar membrane, is affected by mutations of vacuolar SNARE and phospholipase in Arabidopsis. *Plant Journal*, **68**, 64–73.
- Santiago, J., Henzler, C. & Hothorn, M. (2013) Molecular mechanism for plant steroid receptor activation by somatic embryogenesis co-receptor kinases. *Science*, **341**, 889–892.
- Schwacke, R., Schneider, A., van der Graaff, E., Fischer, K., Catoni, E., Desimone, M. *et al.* (2003) ARAMEMNON, a novel database for Arabidopsis integral membrane proteins. *Plant Physiology*, **131**, 16–26.
- Shimada, S., Komatsu, T., Yamagami, A., Nakazawa, M., Matsui, M., Kawai, H. *et al.* (2015) Formation and dissociation of the BSS1 protein complex regulates plant development via brassinosteroid signaling. *Plant Cell*, **27**, 375–390.
- Sun, Y., Fan, X.Y., Cao, D.M., Tang, W., He, K., Zhu, J.Y. *et al.* (2010) Integration of brassinosteroid signal transduction with the transcription network for plant growth regulation in Arabidopsis. *Developmental Cell*, **19**, 765–777.
- Surina, S., Yamagami, A., Miyaji, T., Chagan, Z., Chung, K.M., Mitsuda, N. *et al.* (2024) BIL9 promotes both plant growth via BR signaling and drought stress resistance by binding with the transcription factor HDG11. *Plant & Cell Physiology*, **65**, 1640–1654.
- Tang, W., Kim, T.W., Osés-Prieto, J.A., Sun, Y., Deng, Z., Zhu, S. *et al.* (2008) BSKs mediate signal transduction from the receptor kinase BRI1 in Arabidopsis. *Science*, **321**, 557–560.
- Tang, W., Yuan, M., Wang, R., Yang, Y., Wang, C., Osés-Prieto, J.A. *et al.* (2011) PP2A activates brassinosteroid-responsive gene expression and plant growth by dephosphorylating BZR1. *Nature Cell Biology*, **13**, 124–131.
- Trifinopoulos, J., Nguyen, L.T., von Haeseler, A. & Minh, B.Q. (2016) W-IQ-TREE: a fast online phylogenetic tool for maximum likelihood analysis. *Nucleic Acids Research*, **44**, W232–W235.
- Tsutsui, H. & Higashiyama, T. (2017) pKAMA-ITACHI vectors for highly efficient CRISPR/Cas9-mediated gene knockout in *Arabidopsis thaliana*. *Plant & Cell Physiology*, **58**, 46–56.
- Wang, R., Liu, M., Yuan, M., Osés-Prieto, J.A., Cai, X., Sun, Y. *et al.* (2016) The Brassinosteroid-activated BRI1 receptor kinase is switched off by dephosphorylation mediated by cytoplasm-localized PP2A B' subunits. *Molecular Plant*, **9**, 148–157.
- Wang, R., Wang, R., Liu, M., Yuan, W., Zhao, Z., Liu, X. *et al.* (2021) Nucleocytoplasmic trafficking and turnover mechanisms of BRASSINAZOLE RESISTANT1 in *Arabidopsis thaliana*. *Proceedings of the National Academy of Sciences of the United States of America*, **118**, e2101838118.

- Wang, X. & Chory, J.** (2006) Brassinosteroids regulate dissociation of BK1, a negative regulator of BRI1 signaling, from the plasma membrane. *Science*, **313**, 1118–1122.
- Wang, Z.Y., Nakano, T., Gendron, J., He, J., Chen, M., Vafeados, D. et al.** (2002) Nuclear-localized BZR1 mediates brassinosteroid-induced growth and feedback suppression of brassinosteroid biosynthesis. *Developmental Cell*, **2**, 505–513.
- Wang, Z.Y., Seto, H., Fujioka, S., Yoshida, S. & Chory, J.** (2001) BRI1 is a critical component of a plasma-membrane receptor for plant steroids. *Nature*, **410**, 380–383.
- Wu, G., Wang, X., Li, X., Kamiya, Y., Otegui, M.S. & Chory, J.** (2011) Methylation of a phosphatase specifies dephosphorylation and degradation of activated brassinosteroid receptors. *Science Signaling*, **4**, ra29.
- Xue, X., Wang, L., Huang, A., Liu, Z., Guo, X., Sang, Y. et al.** (2024) Membrane-associated NRPM proteins are novel suppressors of stomatal production in *Arabidopsis*. *Current Biology*, **34**, 881–894.e887.
- Yin, Y., Vafeados, D., Tao, Y., Yoshida, S., Asami, T. & Chory, J.** (2005) A new class of transcription factors mediates brassinosteroid-regulated gene expression in *Arabidopsis*. *Cell*, **120**, 249–259.
- Yin, Y., Wang, Z.Y., Mora-Garcia, S., Li, J., Yoshida, S., Asami, T. et al.** (2002) BES1 accumulates in the nucleus in response to brassinosteroids to regulate gene expression and promote stem elongation. *Cell*, **109**, 181–191.
- Youn, J.H. & Kim, T.W.** (2015) Functional insights of plant GSK3-like kinases: multi-taskers in diverse cellular signal transduction pathways. *Molecular Plant*, **8**, 552–565.
- Yu, X., Li, L., Zola, J., Aluru, M., Ye, H., Foudree, A. et al.** (2011) A brassinosteroid transcriptional network revealed by genome-wide identification of BES1 target genes in *Arabidopsis thaliana*. *Plant Journal*, **65**, 634–646.